Environmental Science Nano

Accepted Manuscript

This article can be cited before page numbers have been issued, to do this please use: Z. Chen, Y. Liu, W. Wei and B. Ni, *Environ. Sci.: Nano*, 2019, DOI: 10.1039/C9EN00411D.

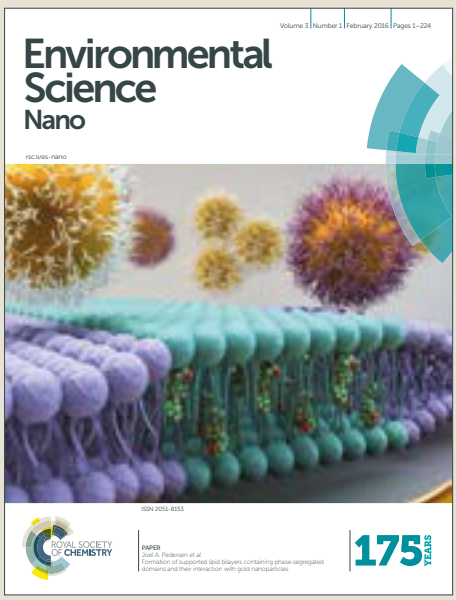

ROYAL SOCIETY OF CHEMISTRY

rsc.li/es-nano

View Article Online
DOI: 10.1039/C9EN00411D

Environmental significance

Electrocatalysis is an efficient approach for the degradation of halogenated organic pollutants. Currently, both electrooxidative and electroreductive dehalogenation processes are widely applied, and the key challenge lies in the development of high-performance electrocatalysts. Given the rapid advances in the design and development of efficient catalysts towards electrochemical dehalogenation, this review aims to summarise recent progress in popular electrocatalysts and theoretical understanding of dehalogenation processes. Additionally, several key prospects in this field are presented. This critical review can facilitate the design and application of next-generation electrocatalysts with ameliorated performances.

DOI: 10.1039/C9EN00411D

Recent Advances in Electrocatalysts for Halogenated Organic Pollutants Degradation

Zhijie Chen, Yiwen Liu, Wei Wei, Bing-Jie Ni*

Centre for Technology in Water and Wastewater, School of Civil and Environmental Engineering, University of Technology Sydney, Sydney, NSW 2007, Australia

*Corresponding author:

Tel.: +61 295147401; E-mail: bingjieni@gmail.com (Prof. Bing-Jie Ni)

View Article Online
DOI: 10.1039/C9EN00411D

Abstract

Electrocatalysis has recently been extensively employed for the degradation of halogenated organic pollutants (HOPs) that normally act as persistent, toxic, and bioaccumulative substances in the environment and pose threats to aquatic species as well as human beings. This review article broadly gives the up-to-date status on promising electrocatalysts for the degradation of HOPs, with particular emphasis on the strategies for promoting the activities of catalysts. Firstly, the catalysts for oxidative mineralization process including metallic oxides- and carbon-based anodes, as well as the oxidative dehalogenation mechanism of these catalysts, are comprehensively presented. Secondly, the catalysts for reductive degradation process, which contains metal- and metal complexes-based cathodes, with their applications and organic transformation pathways, are fully analyzed. Thirdly, recent advances in the integrated techniques are introduced, and the integration of membrane techniques, biological methods, Fenton processes, photocatalysis with electrocatalysis are discussed. Finally, several key directions for further research are exploited, which includes catalysts design, experimental optimization, scientific understanding exploration, and effective coupling techniques.

1. Introduction

Halogenated organic compounds, namely organics containing one or more elements of fluorine (F), chlorine (Cl), bromine (Br) and iodine (I), have aroused increasing concerns as it poses threat to aquatic species as well as human beings. These organics are widely employed in many industrial and consumer products such as pesticides, flame retardants, fungicides, insecticides, dyes, dielectrics, coolants, plant regulators, plasticizers, and drugs.[1-4] Due to their high consumptions during past years, these compounds have been detected in air, water, and soil, which result in severe environmental pollution owing to their high toxicity, persistence, bioaccumulation, and wide distribution.[4, 5]

Under such circumstance, effective methods to degrade these halogenated organic pollutants (HOPs) are extremely demanding. In the last few decades, extensive efforts have been devoted to the degradation of HOPs. Particularly, many processes have been developed to cleave the strong C-X bonds (X= F, Cl, Br and I) in HOPs, such as microbial degradation,[6, 7] ionizing radiation,[8, 9] metallic reduction,[10-12] photochemistry and photocatalysis,[13-15] sonolysis,[16, 17] and electrocatalysis[18-21]. Although it is highly difficult to compare the efficiency of different degradation methods due to various target pollutants, initial concentrations, source of pollution, experimental setups and different physicochemical parameters of these processes applied,[22] electrocatalysis distinguishes itself from these methods for its easy implementation, high energy efficiency, amenability of automation and safety, versatility, high effectiveness, universal degradation capability, as well as environmental compatibility.[1, 23-26]

As a destructive technology for HOPs degradation,[27] especially for those persistent perfluorinated compounds (PFCs), electrocatalysis has attracted much more attention recently.[28] Several previous publications have discussed the application of electrocatalysis in the dehalogenation process.[1, 2, 28-32] For example, Sandra et al.[1] reviewed the electroreduction of organic halides in terms of electrode reaction mechanisms, electrode materials as well as process operation. Martin et al.[2] considered many vital aspects of the electroreduction process of HOPs, including cell designs, experimental methods, and degradation mechanisms. In an earlier work by the same group, the electrochemical reduction of halogenated organic compounds was also discussed regarding the species of pollutants.[32] Apart from electrochemical reduction, Niu and coworkers[28] reviewed the electrooxidation of perfluorinated compounds, and the major focus was on the electrode types and operational factors, including potential, current density, pH value, plate distance, and etc. These informative articles have provided an overview of the electrocatalytic degradation processes

of HOPs related to reduction or oxidation, however, the catalysts applied in this field have not been comprehensively reviewed. In fact, it is now widely recognized that electrocatalysts (electrodes) play a key role in the degradation of HOPs,[33, 34] and explosive development of innovative catalysts are pushing the boundaries of HOPs degradation speedily during past years. Nevertheless, to date, there is no attempt has been made to provide a comprehensive summary of these recent findings to facilitate the development of new effective catalysts.

Therefore, in this review article, we summarize the recent development in electrochemical dehalogenation catalysts, focusing on the key strategies for promoting the activities of catalysts, as well as the connections between the nature of catalysts (such as morphology, chemical component, conformation) and their catalytic performance. In addition, the key mechanisms accounting for electrooxidative dehalogenation (EOD) and electroreductive dehalogenation (ERD) are highlighted, as well as the advanced integrated techniques. Based on the review, the outlooks on key future research directions are also pointed out.

2. Catalysts for electrooxidative dehalogenation

Electrooxidation has been proved as an effective method to mineralize halogenated organic pollutants. To date, numerous catalysts have been applied in the electrooxidative dehalogenation process. This section provides an overview of the main catalysts (anodes) in EOD, including metal oxides (PbO_2, SnO_2, and others)-based and carbon (boron-doped diamond and others)-based electrodes. The diverse modification strategies that have been applied to upgrade the performance of these electrodes are also highlighted. Furthermore, the main electrooxidative dehalogenation mechanisms are discussed.

2.1. PbO_2-based catalysts

PbO_2-based catalysts have been widely explored as the electrode materials in EOD since they possess many merits, including low cost, high conductivity, chemical resistance, as well as

high oxygen overvoltage.[23, 33, 35] Table 1 summarizes the recently representative studies of the EOD by various PbO_2-based catalytic materials. These results clearly suggested that the structure and components of the catalysts have a vital influence on their degradation performance. The effective measures that can upgrade the catalytic potential of PbO_2-based catalysts are detailed in this work.

Pristine PbO_2 materials are excellent candidates for EOD due to their high catalytic activity, good chemical stability, great conductivity, as well as low cost.[36] Normally, the traditional PbO_2 coated catalysts can flake from the substrate (e.g., Ti sheets) for their relatively large interface resistance.[28] To address this problem, interlayers have been introduced to increase the chemical stability and thus the degradation performance of PbO_2 electrode.[36-38] For example, Niu et al.[38] used SnO_2-Sb as an interlayer to construct a Ti/SnO_2-Sb/PbO_2 anode with the electrodeposition method for the decay of perfluorooctanoic acid (PFOA). The degradation of PFOA followed pseudo-first-order kinetics and the degradation efficiency on Ti/SnO_2-Sb/PbO_2 anode achieved 91.1%, with the defluorination rate of PFOA being 77.4%. Recently, the same group found that TiO_2 nanotubes arrays (TNAs*) performed better than SnO_2-Sb when worked as a transition layer for the defluorination of fluoxetine (FLX).[39] They noticed that the particles on the Ti/TNAs*/PbO_2 anode are smaller and distributed much more compactly than that of the Ti/SnO_2-Sb/PbO_2 and Ti/ PbO_2 anodes (Fig. 1 a-c). Impressively, the optimized electronic transport through the "T-shaped" electrode (Fig.1 d) and the improved hydroxyl radical yield derived from selective PbO_2 crystal face growth could facilitate the degradation process (Fig. 1 e-f). Other than metallic oxides, a graphene nanosheet was also employed as an interlayer to construct a novel PbO_2 electrode (GNS-PbO_2) for degradation of 2-chlorophenol (2-CP).[36] The GNS-PbO_2 displayed better electrochemical activities, a higher dehalogenation rate constant and better service lifetime than those of the conventional PbO_2 electrode.

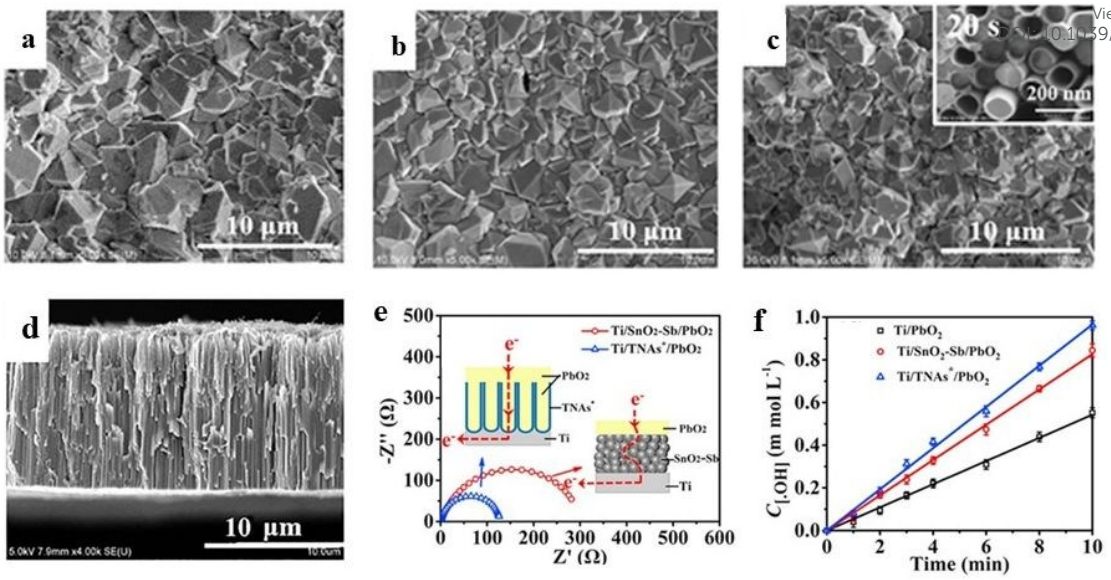

Fig.1 SEM images of Ti/PbO_2 (a); Ti/SnO_2-Sb/PbO_2 (b); Ti/TNAs*/PbO_2 (c); lateral view of TNAs*(d); Nyquist plot of impedance spectra of Ti/SnO_2-Sb/PbO_2 and Ti/TNAs*/PbO_2 anodes in 0.5 mol L^{-1} Na_2SO_4, inset illustrations are the electronic transfer pathways through Ti/TNAs*/PbO_2 and Ti/SnO_2-Sb/PbO_2 anodes(e); concentrations of •OH production on three anodes at the applied current density of 10 mA cm^{-2} (f). Reproduced with permission from ref. 39, Copyright 2018, Elsevier.

However, several defects of pure PbO_2 catalyst have limited its widespread applications, including leaching of toxic Pb ions and relatively large interface resistances.[28, 40] Furthermore, the electrocatalytic activity of bare PbO_2 electrodes still requires further improvements.[38, 41, 42] Therefore, it is crucial to enhance the stability and electrocatalytic activity of PbO_2 electrodes, with doping, compositing, and surface modification being reported as efficient ways to achieve the goal.[40, 43-45] To date, many foreign compositions have been doped on PbO_2 surfaces, such as Bi, Fe, Al, F, Co, Ce, Yb, Gd, Er, La, Au, Zr, Ni, and Sn.[28, 33, 40, 44, 46-49] Among them, Ce is the most used dopant because Ce element can offer PbO_2 a new nucleation center that enhances the electron transfer capacity, minimizes the internal stress of PbO_2 crystals, hampers the further growth of PbO_2 and decreases its average size.[23, 28] Hence, the Ce-doped PbO_2 catalysts display upgraded electrocatalytic performance towards HOPs.

View Article Online
DOI: 10.1039/C9EN00411D

For example, a well-designed TiO_2-NTs/Ce-PbO_2 electrode was prepared for the elimination of Rhodamine B (RhB).[23] Compared to TiO_2-NTs/PbO_2 electrode, the incorporation of Ce favored the generation of a denser and smoother film, with decreased crystal size, as well as a higher exposure of preferred crystalline orientation. The small crystals provided more active sites for electrochemical oxidation, and the dense film hindered the penetration of electrolytes. The abundant active sites and great durability results from the Ce-doping improve the overall electrochemical performance. Recently, metals other than Ce have gained more attention as efficient dopants in the fabrication of PbO_2-based electrodes due to their better dehalogenation capabilities. As a good example, in the mineralization of enrofloxacin (ENR), Wang and coworkers[43] found that Ti/SnO_2-Sb/La-PbO_2 electrode was much more compact than Ti/SnO_2-Sb/Ce-PbO_2 and Ti/SnO_2-Sb/PbO_2 electrodes (Fig.2 a-c), and La doping significantly reduced the crystallite size of β-PbO_2 (Fig. 2 d). Accordingly, the La-doped materials may provide more active sites for the generation of radicals. As a result, these characteristics of La-doped electrode showed better degradation performance (Fig. 2 e-f).

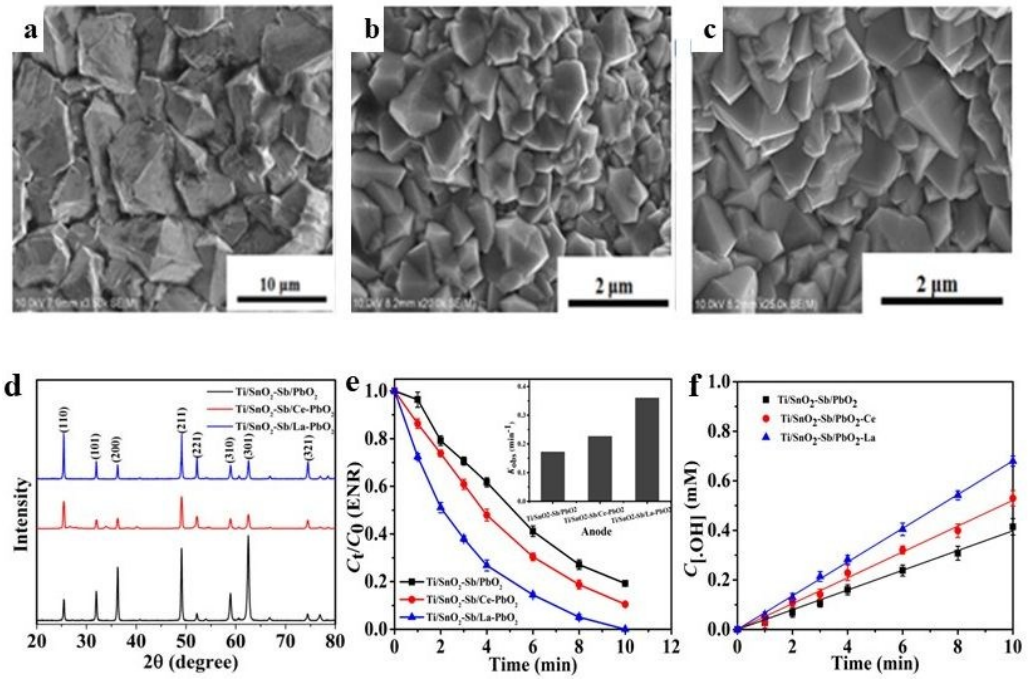

Fig.2 SEM images of the top of Ti/SnO_2-Sb/PbO_2 (a); Ti/SnO_2-Sb/Ce-PbO_2 (b); Ti/SnO_2-Sb/La-PbO_2 (c), XRD patterns of Ti/SnO_2-Sb/PbO_2, Ti/SnO_2-Sb/Ce-PbO_2 and Ti/SnO_2-Sb/La-PbO_2 electrodes (d), electrochemical degradation of 10.0 mg L^{-1} ENR (e) and the concentrations of hydroxyl radicals production by using Ti/SnO_2-Sb/PbO_2, Ti/SnO_2-Sb/Ce-PbO_2 and Ti/SnO_2-Sb/La-PbO_2 electrodes (f). Reproduced with permission from ref. 43, Copyright 2017, Elsevier.

Composting is another useful strategy to obtain a significant leap in the dehalogenation performance of catalysts since composite-based electrodes possess a superior lifetime, high HOP, great chemical stability, as well as excellent degradation power.[50] For PbO_2, the commonly employed incorporating metal oxides include CeO_2, ZrO_2, Co_3O_4, RuO_2, and TiO_2.[51] Among these, the PbO_2-CeO_2 composite electrode is a powerful candidate for EOD.[34, 45, 46] This composite is usually fabricated using a composite electrodeposition method, which can obtain higher cerium contents than the aforementioned Ce-PbO_2 electrode.[34, 45] Therefore, the electrocatalytic ability and chemical stability of PbO_2-CeO_2 composite electrode are higher than that of Ce-PbO_2 electrode.[45] A novel three-dimensional PbO_2-CeO_2 composite electrode was fabricated with a composite electrodeposition method using oxygen bubbles as a template.[34] The 3D/PbO_2-CeO_2 composite electrode possessed a three-dimensional interconnected porous structure, and the CeO_2 nanoparticles were observed on pore walls. Moreover, the composite electrode owned noteworthy capability in hydroxyl radicals generation resulting from the high OEP as well as the high specific surface area, with thiamethoxam being completely mineralized into CO_2 and H_2O after electrolysis for 90 min. Alternatively, PbO_2-ZrO_2 and Ga_2O_3-PbO_2 have also been employed to remove HOPs successfully.[52, 53]

Hydrophobic properties of anodes also have a significant impact on the OEP and the production of •OH radicals that are the main active components in EOD process. Thus

regulating the surface property of PbO_2 from hydrophilic to hydrophobic is greatly advisable.[41, 54] Consequently, the surfactants and polymers are widely applied as additives to upgrade the surface properties of anodes. For instance, a PbO_2 electrode modified with hydrophobic polyvinylidene fluoride (PVDF) was employed to degrade PFOA, and experimental results illustrated that the designed electrode still kept the β-PbO_2 crystallographic structure.[37] The PVDF modified anode exhibited a rough face and the small particles were uniformly distributed. The nanostructures could significantly improve the specific area, and provide abundant reactivity points for the generation of hydroxyl radicals. The presence of PVDF also enhanced the hydrophobicity and the lifetime of the bare PbO_2 electrode. Correspondingly, the Ti/SnO_2-Sb_2O_5/PbO_2-PVDF anode showed a higher degradation efficiency of PFOA than the Ti/SnO_2-Sb_2O_5/PbO_2.

The particle size of catalysts also affects the electrocatalytic performance significantly, and a smaller size is more favorable due to the more active sites for catalytic reactions. Duan and co-researchers[55] fabricated a lauryl benzene sulfonic acid sodium (LAS)-carbon nanotube (CNT)-modified PbO_2 electrode using thermal deposition and electrodeposition methods, and this modified anode exhibited better degradation performance for 4-chlorophenol than the PbO_2 electrode. It was found that the crystal particles on the LAS-CNT-PbO_2 anode were evidently smaller than those on the PbO_2 anode, and its special surface structure consisted of small "stars with four corners" like crystallites. In addition, many bumps appeared on the surface of LAS-CNT-PbO_2 anode, and such feature resulted in a larger effective surface area for the production of active radicals. Totally, these characteristics of surface morphology and coating composition play a vital role in enhancing the capacity of the anode.

Table 1 Summary of representative HOPs electrooxidative dehalogenation using PbO_2-based anodes in recent years.

Anode	Preparation methods	HOPs	C_{HOP} / mg L^{-1}	electrolyte	current density / mA cm^{-2}	Other parameters	HOP Removal rate/%	COD Removal rate/%	TOC Removal rate/%	Ref.

View Article Online
DOI: 10.1039/C9EN00411D

Ti/TiO_2-NTs/Ag_2O/PbO_2	electrodeposition	perfluorooctane sulfonate	0.0929 mM	1.4 g L^{-1} $NaClO_4$	30	100 mL①; 30 ± 2 °C; 12 $cm^2$②	74.87 (180min)	-	56
Double sided Ti-Pt/β-PbO_2	electrodeposition	ciprofloxacin	50	0.1 M Na_2SO_4	30	6.2 cm^2 and 8.37 cm^2; pH 10; 25 °C	100 (2h)	~75(5h)	57
Ti/TNAs*/PbO_2	anodic oxidation; electrodeposition	fluoxetine	5	0.02 M Na_2SO_4	10	3 cm^2; sequential experiment	94.3	83.1	59
GNS-PbO_2	electrophoretic deposition; electro-deposition	2-chlorophenol	50	0.05 M Na_2SO_4	50	200 mL; 30 °C	95.42 (120min)	55.09 (120min)	36
Ti/-PbO_2/β-PbO_2	electrodeposition	2-chlorophenol	50	0.1 M Na_2SO_4	20	35 °C; 8 cm^2	100 (180 min)	-	37
TiO2-NTs/SnO_2-Sb/PbO_2	anodization; sol-gel technique	flutriafol	-	5 g L^{-1} Na_2SO_4	15	1 L; 25 °C	80.42 (180min)	45.35 (180min)	58
3DEM-PbO_2	sol-gel method; sedimentation and solvent evaporation; electrodeposition	flutriafol	-	0.05 M Na_2SO_4	5	electrochemical filtration reactor; 200 mL; 19.63 cm^2	73.8 (180min)	26.4 (180min)	60
Ti/TiO_2-NTs/SnO_2-Sb/Fe-doped PbO_2	anodization process; thermal deposition; electrodeposition	methylene blue	-	-	-	120 mL; 15.75 cm^2	98 (30min)	96 (30min)	4
Ti/La-Y-PbO_2	electrodeposition	levofloxacin	800	0.1 M Na_2SO_4	30	250 mL; 24 cm^2; pH 3	F^- 93.5 (150min)	-	-
Ti/Yb-PbO_2	electrodeposition	acetamiprid	80	0.05 M Na_2SO_4	250	500 mL; 50 cm^2	98.96 (120min)	74.57 (120min)	-
Ti/SnO_2-Sb/Zr-PbO_2	sol-gel method; electrodeposition	Perfluorooctanoic acid	100	10 mM $NaClO_4$	10	100 mL;96 cm^2; 25 °C; sequential reaction system	>70 (90min)	60 (90 min)	-
Ti/SnO_2-Sb_2O_5/Bi-PbO_2	thermal decomposition; electrodeposition	tebuconazole	12.5	0.01 M $NaClO_4$	40	27 °C	-	-	68 (120 min)
Ti/Sn-SbO_x/Al-PbO_2	thermal deposition; electrodeposition	chloramphenicol	500	0.2 M Na_2SO_4	30	pH 3; 250 mL	87.30 (2.5 h)	-	52.06 (2.5 h)
Ti/SnO_2-Sb/La-PbO_2	sol-gel technique; electrodeposition	enrofloxacin	10	20 mM Na_2SO_4	8	30 mL; 25 cm^2	95.3 (30 min)	-	95.1 (30 min)
Ti/PbO_2-CeO_2	composite electrodeposition	thiamethoxam	30	0.15 M Na_2SO_4	30	500 mL; 6 cm^2; pH 6	100 (90min)	89.0 (90min)	-
Ti/PbO_2-CeO_2	composite electrodeposition	malachite green	30	0.2 M Na_2SO_4	30	100mL; pH 5	95.4 (90min)	69.3 (90min)	-
Ti/Ga_2O_3-PbO_2	sol-gel method; composite plating method	bromocresol green sodium	100 ppm	0.1 M PBS	8	100 mL; 8 cm^2; 40 °C	-	~70 (60min)	-
Ti/RuO_2-SnO_2-TiO_2/PbO_2-CeO_2	sol-gel method; electrodeposition	4-Chlorophenol	100	10 g L^{-1} Na_2SO_4	20	pH 6.7	> 90 (80min)	94.71 % (140min)	-
Ti/SnO_2-Sb_2O_3/PbO_2-ZrO_2	thermal decomposition; pulse electrodeposition	rhodamine B	30	0.2 M Na_2SO_4	200	100 mL; 25 °C	100 (100min)	-	82.9 (100min)
PTFE-doped β-PbO_2	electrodeposition	norfloxacin	100	0.1 M Na_2SO_4	10	500 mL; 11.76 cm^2; 40 °C	100 (12h)	-	70(12h)
Ti/Sn-SbOx/PbO_2-PDMS	thermal deposition; electrodeposition	p-chlorophenol	0.5mM	0.05M Na_2SO_4	20	200 mL	99.0(120min)	-	92.9 (120min)
Ti/SnO_2-Sb_2O_5/PbO_2-PVDF	co-electrodeposition	polyvinylidene fluoride	100	1.4 g L^{-1} $NaClO_4$	30	200 mL; 17.64 cm^2; 26 ± 2 °C	92.1	-	-
Ti/TiO_2-based SnO_2-Sb/FR-PbO_2	anodization; sol-gel method; electrodeposition	ofloxacin	20	0.05 M Na_2SO_4	30	differential column batch reactor; 300 mL; 10 cm^2; pH 6.25	>99 (90min)	--	-
Ti/PTFE-F-CeO_2-PbO_2	electrodeposition	p-chlorophenol	1.0mM	-	100	200 mL; 25 ± 1 °C	48.4 (150min)	20.1 (150min)	-

① initial volume of reaction solution; ② anode area

View Article Online
DOI: 10.1039/C9EN00411D

2.2. SnO_2-based catalysts

SnO_2-based electrocatalysts are frequently used to mineralize HOPs, though SnO_2 is an n-type semiconductor with a band gap of 3.6 eV.[65] To fully expand the range of its applications, doping is the most widely employed strategy to change the intrinsic property of SnO_2 and make it a hotspot in the field of electrode material. Several sophisticated doped SnO_2-based catalysts and their applications are discussed in this work.

Table 2 summarizes the recently representative SnO_2-based catalytic anodes used in the process of HOPs oxidation. It can be found that antimony (Sb) is the most general dopant as Sb-doped anodes possess high OEP, high stability and favorable electrocatalytic characteristics.[66, 67] For instance, a SnO_2-Sb/Ti electrode fabricated with the sol-gel method was employed for the degradation of ciprofloxacin.[68] The coating particles of the anode were uniform in size, with diameters ranging from 20-100 nm. The nanostructure of the SnO_2-Sb/Ti anode exhibited a large surface area, and thereby provided plentiful active sites for the electrocatalytic process. In 120 min, the removal ratios of ciprofloxacin, COD, and TOC were around 99.5%, 86.0%, and 70.0%, respectively.

Components (e.g., F, Ni, Bi, Fe, Ru, Co, Ce, Pd, TiN) often work as co-dopants to improve the performance of Sb-SnO_2 electrode.[65, 69-71] Yang et al. [65] analyzed the effect of six elements (e.g., Fe(III), Ni(II), Co(II), Ru(III), Ce(III), Pd(II)) on the performance of Sb-SnO_2 electrode toward mineralization of Eosin Y. In this study, both Ni and Fe could upgrade the electrocatalytic activities of Sb (5%)-SnO_2, especially Ni. Further study implied that the improvement by Ni doping might be ascribed to the elevated involvement of organic peroxy radicals. Recently, a well-designed F and Sb co-doped SnO_2 anode displayed excellent capacities in the degradation of perfluorooctane sulfonate (PFOS).[69] The co-doped electrode presented better degradation capacities than that of single doped electrodes, and the main

reason was that the formed smooth surface could provide more physically adsorbed •OH radicals and result in relatively high OEP. TiN, as a kind of metal nitride, has been extensively employed as an electrode material due to its unique features, such as relatively low costs, high hardness, good chemical stability, great electric conductivity, and superior catalytic activities.[72, 73] Duan et al. [70] prepared a Ti/Sb-SnO_2-TiN anode for degradation of methylene blue. The TiN-doped anode exhibited a smaller crystal grain size, and thereby boosted the active sites and specific surface area for the electrocatalytic reaction. In addition, the electrochemical impedance spectroscopy tests suggested that the introduction of TiN could obviously decrease the charge transfer resistance (150 ohm vs.1334 ohm), and thus improving the conductivity of the anode. Compared with Ti/Sb-SnO_2, Ti/Sb-SnO_2-TiN had a higher adsorption capacity of hydroxyl oxygen species (1.97 times), as well as a higher decolorization efficiency (1.54 times) and a larger kinetic rate constant (3.24 times).

With good stability and a great electrocatalytic activity, SnO_2-based mixed metal oxide materials are also favourable anodes in the electrocatalytic dehalogenation process.[74] For example, Bai and co-authors [75] designed a Ti/SnO_2-RuO_2 electrode to decompose bromocresol green (BCG) in wastewater. The "cracked-mud" structure electrode showed a high specific surface area, which could provide abundant active sites and enhance the catalytic performance. Under the optimal experimental conditions, the removal ratio of BCG reached 91% within 150 min. Vargas et al. [76] fabricated a SnO_2-Sb_2O_5 anode to mineralize dichlorvos (DDVP) that is a widely used organophosphorus insecticide. The reaction kinetics for DDVP electrochemical oxidation was higher than other advanced oxidation methods (e.g., TiO_2/UV and ZnO/UV), and the COD could be completely removed in about 100 min.

Table 2 Summary of representative HOPs electrooxidative dehalogenation using SnO_2-based anodes in recent years.

Anode	Preparation methods	HOPs	C_{HOP} / mg L^{-1}	electrolyte	current density / mA cm^{-2}	Other parameters	HOP Removal rate/%	COD Removal rate/%	TOC Removal rate/%	Ref.

MI-meso SnO_2	evaporation induced self-assembly	2,4-dichlorophenoxyacetic acid	10 ppm	0.1 M Na_2SO_4	6.34 ± 0.05	100 mL; pH ~7; applied voltage 2.5V	99.15(3h)	-	93.2 (1.5 (3h)	77
Ti/TiHx/Ni-Sb-SnO_2	spin-coating; pyrolysis process	methylene blue	10	0.5 M H_2SO_4	50	100 mL; pH 2; 1 cm^2	~100 (10min)	-	-	78
Ti/Sn-Sb/SnO_2-F-Sb	electrodeposition; sol-gel	perfluorooctane sulfonate	100	10 mM $NaClO_4$	20	50 mL; pH 3; 25 ± 3 °C	>99 (120min)	-	-	69
Ti/SnO_2-RuO_2	thermal decomposition	bromocresol green	100	4 g L^{-1} Na_2SO_4	12	100 mL; 5 cm^2; pH 7; 30 °C	91 (150min)	-	-	[illegible]
SnO_2-Sb/Ti	sol-gel method	ciprofloxacin	50	0.05 M Na_2SO_4	30	250 mL; 15 cm^2; 30 °C	99.5 (120min)	86.0 (120min)	70.0 (120min)	68
Ti/Ta_2O_5–SnO_2	thermal decomposition; drop casting	methylene blue	0.1 mM	0.1 M Na_2SO_4	9	2.2 cm^2; pH 6.5; 25 ± 2 °C	95(2h)	85(2h)	-	[illegible]
Ti/SnO_2–F	sol-gel method; dip coating;	perfluorooctanoic acid	100	10 mM $NaClO_4$	20	50 mL; 30 cm^2; 25 ± 3 °C	>99 (30min)	-	92.6 (30min)	[illegible]
Ti/SnO_2–Sb_2O_5–Bi_2O_3	sol-gel method	1H,1H,2H,2H-perfluorooctane sulfonic acid	20	1.4 g L^{-1} $NaClO_4$	6.8	200 mL; 30 cm^2; 32 °C; 0.4% CH_3OH as the co-solvent	23.8 (3.5h)	-	-	81
SnO_2-Sb_2O_5	-	2,2-dichlorovinyl dimethyl phosphate	15	0.1 M Na_2SO_4	-	50 mL; 1 cm^2; 25 ± 3 °C	-	~100 (100min)	-	[illegible]
Ti/Sb-SnO_2-NGNS	sol-gel method; dip coating	methylene blue	50	0.25 M Na_2SO_4	20	50 mL; 2 cm^2	97.7 (100min)	-	-	[illegible]
Ti/Sb–SnO_2–TiN	pulse electro-codeposition	methylene blue	50	0.25 M Na_2SO_4	20	50 mL; 2 cm^2	100 (120min)	-	-	70
SnO_2-Sb/CA	sol-gel method; solvent exchange; ambient pressure drying; pyrolysis	perfluorooctanoate	100	0.1 M Na_2SO_4	20	60 mL; 5 cm^2	91(5h)	-	86(5h)	83
Ti/Ni–Sb–SnO_2	dipping-coating	Eosin Y	1 mM	0.1 M Na_2SO_4	22.22	20 mL; 4.5 cm^2	~48 (25min)	-	~75(2.5h)	[illegible]
Ti/SnO_2-Sb-Bi	sol-gel method	perfluorooctanoate	50	1.4 g L^{-1} $NaClO_4$	22.07	25 mL; 11.33 cm^2	>99 (2h)	-	-	67
Mo-SnO_2/BDD	anodic treatment; sol-gel technique	clofibric acid	200	0.05 M Na_2SO_4	30	4 cm^2; 100 mL; 25 ± 2 °C;	95 (240min)	90 (240min)	-	[illegible]

2.3. Other metal oxide-based catalysts

Like the oxides of Pb and Sn, other metal oxides (e.g., RuO_2, Bi_2O_3, IrO_2, Ti_4O_7) are also employed as electrodes in recent years owing to their relatively low cost, high chemical stability and superior electrocatalytic activities.[85, 86] Table 3 collects the recently representative studies involve the electrochemical oxidation of HOPs by metal oxides (except PbO_2 and SnO_2)-based catalytic materials. Among these, RuO_2- and Ti_4O_7- based electrodes are underlined in this work as two typical examples.

RuO_2 has emerged as a promising candidate for mineralization of HOPs owing to its high stability, high OEP, great electrochemical performance and low cost.[86, 87] In addition, RuO_2 showed high capacity toward the generation of active oxidants such as chlorine, ozone, and free radicals.[88] Kaur and co-authors [86] used the Ti/RuO_2 anode to decay ofloxacin antibiotic

View Article Online
DOI: 10.1039/C9EN00411D

(OFLX), and experimental results suggested that H_2O_2, HO_2•, HOCl, ClO^- and chemisorbed •OH are all active components in the degradation process. As a result, removal ratios of OFLX and TOC were about 80% (30 min) and 46.3% (240 min), respectively. To enhance the performance of RuO_2 anode through enlarging the electrochemical surface area, Zhang et al. [89] fabricated a tubular porous Ti-RuO_2 electrode and designed a corresponding reactor to degrade anticancer drugs wastewater containing 5-Fluoro-2-Methoxypyrimidine (5FMP). The electrode with a porous structure had larger active surface area than the plate electrode with the same geometrical area. Additionally, the micro-sized pores of Ti-RuO_2 electrode achieved a vertical flow between the anode and cathode in the presence of the pump. As a result, the designed reactor could not only improve the mass transfer process but also generate a homogeneous velocity distribution and high turbulent mixing around the electrode. For these merits, the 5FMP was completely removed and the removal efficiency of COD reached 84.1%, within 180 min of electrocatalysis.

Ti_4O_7 that is a Magnéli phase titanium sub-oxide has been suggested as a good candidate for electrodes owing to its great conductivity (~1000 S cm^{-1}), high OEP (2.6 V/SHE, standard hydrogen electrode), good chemical stability, and easy preparation.[90-92] Therefore, Magnéli phase Ti_4O_7 ceramic materials have been widely worked as anodes in the electrochemical purification of wastewater. Lin et al. [92] found that the macroporous Magnéli phase Ti_4O_7 ceramic materials possessed interconnecting macropores, with size ranging within 1-8 μm (Fig. 3 a-d). Compared to Ce-PbO_2 and BDD anodes, the porous Ti_4O_7 ceramic electrode had a greater surface area and the enhanced interphase mass transfer, thus improving the overall current efficiency. As a result, the porous anode exhibited better performance than Ce-PbO_2 and BDD anodes in the mineralization of poly- and perfluoroalkyl substances (Fig. 3 e-f). Additionally, previous work reported that Co_3O_4,[93] IrO_2,[94] and Bi_2O_3[85, 95] are also excellent

candidates for the EOD process, owing to their favourable electrochemical activities, good mechanical and chemical resistance.[95]

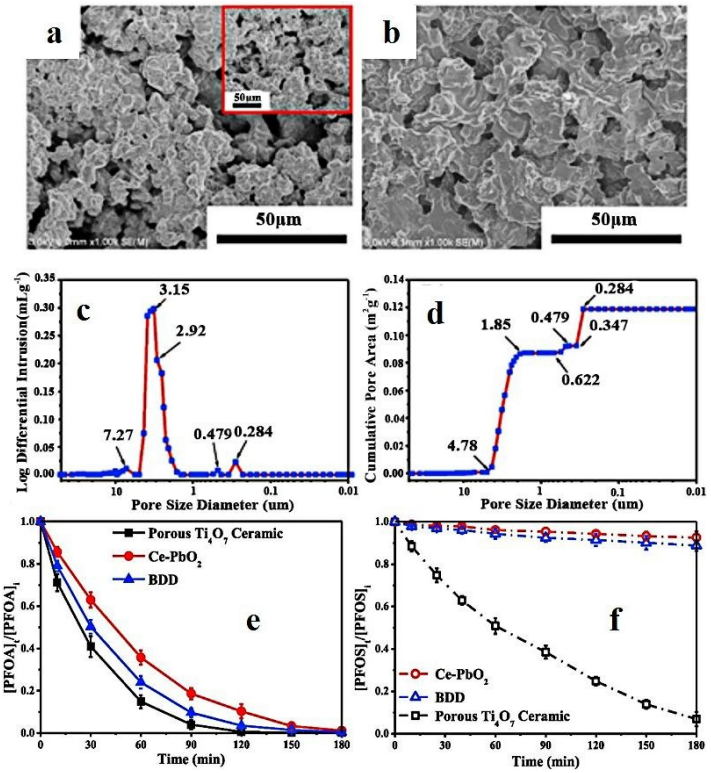

Fig.3 SEM image of the surface (a) and cross-section (b) of the macroporous Magnéli phase Ti_4O_7 ceramic plate materials; (c, d) results of Hg intrusion porosimetry analysis of pore size distribution; concentration change of 0.5 mM PFOA (e) and 0.1 mM PFOS (f) during electrooxidation process by different anodes. Reproduced with permission from ref. 92, Copyright 2018, Elsevier.

Table 3 Summary of representative HOPs electrooxidative dehalogenation using metal oxides (except PbO_2 and SnO_2)-based anodes in recent years.

Anode	Preparation methods	HOPs	C_{HOP} / mg L^{-1}	electrolyte	current density/ mA cm^{-2}	Other parameters	HOP Removal rate/%	COD Removal rate/%	TOC Removal rate/%	Ref.
Ti/RuO_2	-	ofloxacin	50	2 g L^{-1} NaCl	-	1.5 L; pH 6.8 ± 0.1; 1 A	~80 (30 min)	-	46.3 (240min)	[redacted]
Ti/RuO_2-IrO_2	-	4-chlorophenol	50 ppm	1 g L^{-1} NaCl	25	32 cm^2; 1 L; pH 7.38;	57.61 (89 min)	-	-	[redacted]
tubular porous Ti-RuO_2	sol–gel technique; thermal decomposition	5-Fluoro-2-Methoxypyrimidine	61.2	-	5	94.2 cm^2; 1 L; pH 5.0; flow rate 0.31 L min^{-1},	100	84.1	-	89
RuO_2–PdO–TiO_2/Ti	sol–gel; dip-coating	rhodamine B	1.043× 10^{-5} M	1.709× 10^{-3} M NaCl	-	0.5 L; 0.02 A	-	71.70 (30 min)	-	97
RuO_2-coated Ti	-	rhodamine 6G	200	0.2 M NaCl	16.52	300 mL; 115 cm^2; 25 °C; pH 2	>99	>90	-	88
Ti/RuO_2	thermal	oxytetracycline	2.01× 10^{-3}	0.80 M	50	2 cm^2; pH 5.45	100	-	-	98

View Article Online
DOI: 10.1039/C9EN00411D

	decomposition	hydrochloride	M	phosphate buffer			(120 min)	-	-	
Co_3O_4 nanowires/carbon cloth	-	triclosan	40	1M KOH	10	6 cm^2	95 (60 min)	-	-	93
Ti/IrO_2	-	norfloxacin	62.6 μM	5× 10^{-2} M NaCl	6.53	150 mL; 3.06 cm^2; pH 9.0	100 (20 min)	-	-	94
Ti-Bi_2O_3	galvanostatic electrodeposition	Reactive Orange 4	0.32 mM	10 mM H_2O_2; 10 mM Na_2SO_4	40	20±0.5 °C; pH 7	100 (40min)	-	-	95
stainless steel/Bi_2O_3	electrodeposition; calcination	Methylene blue	0.08 mM	10 mM H_2O_2; 10 mM Na_2SO_4	40	20±0.5 °C; pH 7±0.2	100 (125min)	-	-	96
stainless steel/Bi_2O_3	electrodeposition; calcination	Reactive Orange 4	0.08 mM	10 mM H_2O_2; 10 mM Na_2SO_4	40	20±0.5 °C; pH 7±0.2	100(35min)	-	-	85
Au/Bi_2O_3	electrodeposition	Crystal violet	50	10 mM H_2O_2; 1 mM Na_2SO_4	10	pH 7±0.1	100 (20min)	-	-	99
porous Ti_4O_7 ceramic	high-temperature sintering	perfluorooctanoate	0.5 mM	20 mM $NaClO_4$	5	50 cm^2; 250 mL; 25±1 °C	>99.9 (180min)	-	>95 (180min)	92
porous Ti_4O_7 ceramic	high-temperature sintering	perfluorooctanesulfonate	0.1 mM	20 mM $NaClO_4$	5	50 cm^2; 250 mL; 25±1 °C	93.1 ± 3.4 (180min)	-	90.3 ± 1.8 (180min)	92

2.4. Carbon-based catalysts

Anode materials derived from carbon have also been extensively employed in the EOD process since these electrodes own excellent chemical stability together with low resistivity. The widely reported carbon-based catalysts include BDD,[21, 100, 101] graphite,[20, 102] activated carbon fiber,[103] carbon nanotubes,[104, 105] and granular activated carbon[26, 106]. The catalytic performance of representative carbon-based anodes for HOPs degradation is presented in Table 4. Among these carbon-based anodes, BDD is the most widely explored one due to its distinct advantages over other anodes, such as high corrosion resistance, favorable electrochemical stability, high OEP (2.8 V/SHE), a wide electrochemical potential window, and a low background current.[107] Numerous studies suggest that many intrinsic properties of BDD anodes and electrochemical experimental conditions have a great impact on the degradation performance of BDD anodes.

BDD films are usually fabricated with the chemical vapor deposition (CVD) method, and a substrate is necessary to support the BDD film and improve its stability.[108-110] The commonly used substrates include Si, Ta, Ti, Nb, and W, but it is difficult to evaluate the stability of

View Article Online
DOI: 10.1039/C9EN00411D

BDD films as a function of substrate type due to the non-uniform preparation parameters among different studies, as well as evident pros and cons of each substrate.[108] Apart from the substrate, another intrinsic property that can heavily influence the electrocatalytic performance of BDD is the sp^3 (diamond)/sp^2 (graphite) carbon ratio.[111-115] For example, six p-Si BDD anodes with different sp^3/sp^2 carbon ratios (165-323) showed various degradation capacities towards 2, 4-dichlorophenoxyacetic acid (2, 4-D).[112] A more speedy and effective dechlorination of 2, 4-D is due to a higher sp^3 carbon content in the BDD anode. However, the sp^3/sp^2 ratio has no effect on the type of detected intermediates. On the other hand, Araújo and co-authors [114] found that more aromatic intermediates are formed at the BDD_6 anode (high sp^3 carbon), while less of them are yielded when BDD_1 anode (high sp^2 carbon) was used, in the mineralization of RhB. Their further exploration indicated that a higher content of sp^3 carbon resulted in greater TOC and COD decomposition by electrochemical mineralization with hydroxyl radicals. In contrast, BDD anode with a lower sp^3/sp^2 ratio favoured the electrochemical conversion (formation of many intermediates) because of the strong adsorption of reactants on graphite carbon sites. In other words, sp^2 carbon species behave as "active anode" parts, which mainly follow the direct oxidation process and leads to a lower RhB combustion ratio. More details about this aspect can be found in previous reviews.[111, 113]

To further upgrade the electrochemical oxidation performance of the planar/bare BDD anodes, the surface modification is highly recommended.[116, 117] Nanocrystallizing,[118] chemical etching,[119] electrochemical anodizing,[120, 121] porous structuring,[122, 123] and hybridizing[116, 123] are proved as the efficient strategies to achieve better electrochemical performance of BDD electrodes. The general idea of these methods is to improve the active surface area, enhance the intrinsic electrochemical activity and boost the durability of electrodes.[123] Urtiaga et al.[118] employed an ultrananocrystalline boron doped conductive

diamond electrode that possessed a thin film coating and nanoscale grain size to degrade PFOA (100 mg•L^{-1}). Several key experimental parameters were investigated systematically, including the supporting electrolyte, the applied current density and the hydrodynamic conditions. The results suggested that PFOA degradation and mineralization ratios were higher than 90% within 6 hours, at an applied current density of 200 A•m^{-2}. Currently, the applications of modified BDD in the mineralization of HOPs are rarely reported, and more attention should be encouraged to make higher use of these great BDD electrodes.

In the EOD process, the supporting electrolyte has a conspicuous influence on the mineralization performance of BDD anodes. Specifically, the degradation kinetics and efficiency, as well as the degradation pathways are sensitive to electrolytes.[124-126] The commonly used electrolytes include NaCl, Na_2SO_4, $NaNO_3$, and $NaHCO_3$. Among these, NaCl and $NaSO_4$ are the most attractive ones since they can produce highly effective hydroxyl radicals, such as Cl•, ClO_x•, $SO_4^{\bullet-}$, and $S_2O_8^{2-}$, which are beneficial to the decay of HOPs.[127, 128] Carneiro et al.[125] compared the effect of five different electrolytes (Na_2SO_4, NaCl, Na_2CO_3, $NaNO_3$, Na_3PO_4) on the removal of enrofloxacin, using a BDD anode. Compared to other electrolytes, NaCl led to an appreciably faster degradation of enrofloxacin, and the most initial intermediates were chlorinated. Nevertheless, Na_2SO_4 manifested a better performance than NaCl in the electrooxidation of losartan with a BDD electrode.[126] Using Na_2SO_4 as supporting electrolyte, the mineralization ratio (67%) was higher than that of the NaCl system (56%). Interestingly, Mena et al.[127] designed an experiment to clarify the contribution of hydroxyl radicals and electrogenerated sulfur-based radicals (e.g., peroxodisulfate) in the degradation of three different ionic liquids (ILs) using a BDD anode. Their results suggested that sulfate could improve the efficiency of the electrooxidation process and prevent the formation of polymers.

In addition, many studies underscore the importance of the water matrix on the EOD process with BDD anodes.[129-131] Naturally, waters contain various organic and inorganic, non-target components. These constituents may interact with the oxidizing radicals and the target pollutants. As a result, the presence of these chemicals can heavily impact the performance of BDD anodes. The frequently investigated components include chloride, sulfates, carbonates, and humic acid. As aforementioned, chloride can introduce different active chlorine species that complement •OH in the mineralization of HOPs. However, a high concentration of Cl^- can improve Cl_2 evolution and hence, cause a reduction of the anode performance. What's worse, several organochlorinated components, such as chloramines and trihalomethanes, may be generated in the electrocatalysis process, which is detrimental to the degradation process owing to their high toxicity and strong recalcitrance.[132, 133] In contrast, radicals derived from sulfates act as good mediators and contribute to the indirect electrocatalysis of pollutants.[129] Conversely, the presence of carbonates/bicarbonates can reduce the mineralization efficiency of BDD anodes, due to the fact that carbonates/bicarbonates are •OH scavengers, namely, carbonates/bicarbonates can consume •OH and reduce the availability of •OH to target HOPs.[132] Humic acid (HA) is an analogue of natural organics typically detected in waters. HA has been recognized as a detrimental component in the degradation of HOPs for several reasons: (1) competition between HA and target HOPs for radicals, (2) HA is a radical scavenger and (3) binding reactions between HA and pollutants.[132]

Other than BDD, carbon nanotubes, activated carbon, and graphite have also been employed in the decay of HOPs. Carbon nanotubes (CNTs) attract enormous attention due to their one-dimensional conduction pathways, chemical stability, good electrical conductivity as well as high surface area.[104, 134] Combined with graphene, the CNTs-graphene composite electrode exhibited excellent performance in the mineralization of perfluorinated compounds (PFCs) owing to the synergy of electrochemical degradation and electrosorption (Fig. 4).[135] Granular

activated carbon (AC) often acts as a particulate electrode in the electrolysis system, which can enhance the overall active electrode area, conductivity, and mass transfer and improve the electrochemical degradation kinetics and COD removal ratio.[136] Pedersen et al. [137] explored the synergy of AC adsorption and electrochemical degradation in the mineralization of 2-methyl-4-chlorophenoxy acetic acid (MCPA) and 2-methyl-4-chlorophenoxy propionic acid (MCPP). Their results indicated that synergies of 121-126% were found for MCPA and MCPP at w/w AC: the organic ratio of 5:1, with an electric field strength of 375 $V \cdot m^{-1}$. Recently, graphite has been employed as an anode for the mineralization of atrazine for the first time.[20] The oxygen-containing functional groups produced by the positively polarized graphite electrode played a catalytic role. The X-ray photoelectron spectroscopy (XPS) analysis verified the presence of oxygen-containing functional groups (C-OH, COOH, and C=O) on the graphite anode surface during the anodic oxidation (water oxidation) process. Surprisingly, no indicator for the production of abundant hydroxyl radicals at graphite electrodes was found, and the atrazine was virtually degraded by the chemisorbed reactive oxygen.

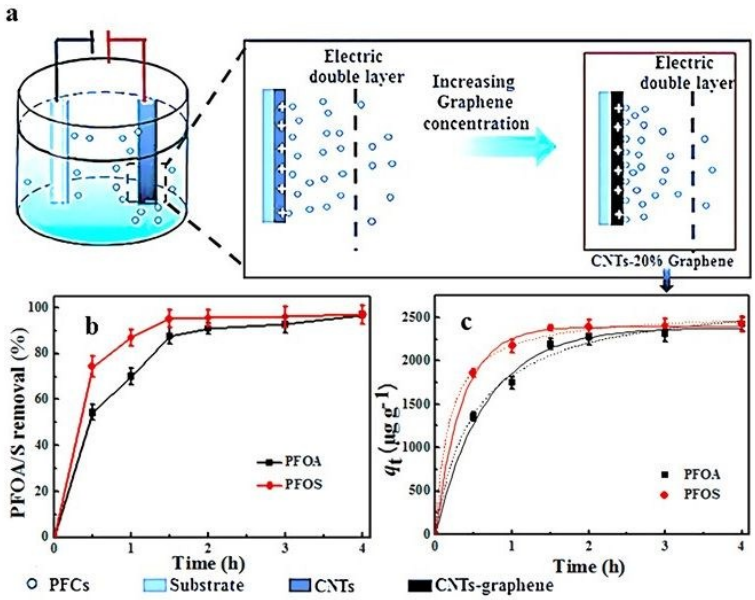

Fig.4 (a) A schematic illustration of the degradation process; the removal ratios (b) and electrosorption kinetics (c) of PFOA and PFOS on CNTs-

20% graphene composite electrode fitted by pseudo-first-order equation (- -) and pseudo-second-order equation (……). Reproduced with permission from ref. 135, Copyright 2017, Elsevier.

Table 4 Summary of representative HOPs electrooxidative dehalogenation using carbon-based anodes in recent years.

Anode	HOPs	C_{HOP} / mg L^{-1}	electrolyte	current density/ mA cm^{-2}	Other parameters	HOP Removal rate/%	COD Removal rate/%	TOC Removal rate/%	Ref.
BDD	norfloxacin	100	2 g·L^{-1} Na_2SO_4	83	250 cm^3	92 (30min)	44 (30min)	-	138
graphite	atrazine	10	0.05 M NaCl	10	300 mL; pH 6.8; 25 ± 2 °C	100 (60min)	-	-	20
BDD (PB/C 500 ppm)	5-fluorouracil	50	6 g·L^{-1} Na_2SO_4	16	200 mL; pH 6.0; 20 °C	100 (6h)	89 (6h)	69 (6h)	21
BDD (PB/C 10000 ppm)	Helectine F ($C_{23}H_{12}Cl_2N_6Na_3O_{10}S_3$)	50	6 g·L^{-1} Na_2SO_4	8.8	flow reactor; 2.3 cm^2; 0.1 L; pH 3.0; 0.6 L h^{-1}	94.9	86.3	-	139
BDD (PB/C 10000 ppm)	Helectine D ($C_{29}H_{16}Cl_1N_7Na_4O_{13}S_4$)	50	6 g·L^{-1} Na_2SO_4	8.8	flow reactor; 2.3 cm^2; 0.1 L; pH 3.0; 0.6 L h^{-1}	94.8	95.7	-	139
BDD	4-chlorophenol	500	0.1 M Na_2SO_4	400	400 mL; pH 6.5; 25 °C	96 (150min)	-	83 (150min)	101
CNTs/AG/ITO	2-chlorophenol	20	-	-	100 mL; pH 2; bias voltage 4 V	98 (180min)	-	-	104
BDD (PB/C 1000 ppm)	thiamethoxam	2	0.1 M Na_2SO_4	16	12.5 cm^2; 150 mL	100 (20min)	-	91 (120min)	132
BDD (PB/C 500 ppm)	ciprofloxacin	69 μM	0.1 M K_2SO_4	7.24	flow reactor; 69 cm^2; 1 L; pH 3.0; 360 L h^{-1}; 30 °C	100 (180min)	-	-	130
MCD BDD	perfluorooctanoic acid	0.24 mM	-	5	70 cm^2; 293 ± 2 K;1 L	100(4h)	-	89(4h)	140
BDD	lindane	0.42	50 mM Na_2SO_4	400	230 mL; 24 cm^2; pH 7.0; 25 °C	100 (4h)	-	90 (4h)	129
BDD (PB/C 100 ppm)	enrofloxacin	100	0.1 M NaCl	10	filter-press flow cell; 23.75 cm^2; 1 L; pH 3.0; 420 L h^{-1}	100 (1h)	-	-	125
BDD	losartan	0.377mM	50 mM Na_2SO_4	10	100 mL; 24 cm^2; pH 7.0; 25 °C	100 (180min)	-	71 (180min)	126
BDD	poly- and perfluoroalkyl substances	1.652	-	50	70 cm^2; 2 L; 3 L min^{-1}; flow-by cell	99.7 (10h)	-	>90 (10h)	141
CNT sponges	perfluorooctanoic acid	0.1	10 mM Na_2SO_4	-	200 mL; 1 cm^2; 25 ± 1 °C; bias voltage 4 V	>90 (180min)	-	-	142
BDD	diquat dibromide	100	-	0.5	300 mL; 100 cm^2; pH 6.5; 25°C; 500 mL min^{-1}	99.17 (5h)	57.64 (5h)	71.31 (5h)	143

Apart from electrochemical activity, the stability of electrocatalysts is another key property in practice. The deactivation of anodes is a common issue in the electrochemical oxidation process, especially the PbO_2 and SnO_2 based catalysts.[33, 37, 39, 68, 70, 78, 90, 144] There are many factors responsible for the anodic deactivation, such as mechanical damages, detachment,

consumption/dissolution, and passivation, as well as operating conditions (e.g., temperature, applied current), etc.[70, 145, 146]

To alleviate the deactivation and prolong the lifetime of catalysts, the efficient strategies (e.g., doping, introducing interlayer) which focus on optimizing the catalyst configuration have exhibited great potentials.[78] Recently, Yu et al.[33] investigated the influence of Ce doping and the RuO_2-SnO_2-TiO_2 interlayer on the stability of the PbO_2 electrode through the accelerated life tests. Three samples, namely PbO_2-0 (unmodified PbO_2/Ti), PbO_2-1(Ti/ RuO_2-SnO_2-TiO_2/PbO_2), and PbO_2-3 (Ti/RuO_2-SnO_2-TiO_2/PbO_2-CeO_2, Ce/Pb = 0.01), exhibited completely different anti-deactivation abilities. The service lifetime of PbO_2-3 was 215 h, which was 0.7 times longer than that of PbO_2-1(125 h) and 9.2 times longer than that of PbO_2-0 (21 h). Consequently, both Ce doping and the existence of the RuO_2-SnO_2-TiO_2 interlayer could notably improve the catalysts' durability. Other than the interlayer, Ce doping could conduce the formation of compact surface layer, which also regulated the durability. The compact surface could effectively hinder the penetration of electrolytes into the Ti substrate and decrease the inner mechanical stress on PbO_2, thus improving the durability. Many similar reports also emphasise the role of doping and interlayer in the construction of robust anodes.[144, 147-149]

2.5. Electrooxidative dehalogenation mechanisms

The successful cleavage of C-X bonds through electrochemical oxidation by catalysts mainly derives from reactive species and/or electrons. Hence, the EOD process can be roughly divided into two categories, namely, direct anodic oxidation and indirect oxidation. It is worth noting that many degradation processes involve both pathways,[38, 65, 150] and the direct oxidation reaction is a vital rate-limiting step for the degradation of pollutants that are unreactive with reactive oxygen species (e.g., fluorinated compounds).[108]

The direct anodic oxidation process occurs directly on the surface of anodes and involves direct electrons transfer between the HOPs and anode surface. Adsorption of organics onto anode surfaces is an important step in this process as it largely determines the degradation rate.[151] Another important factor is the applied potential, and the wanted potential should be higher than that of the H_2O oxidation reaction. Otherwise, the applied electrode is susceptible to surface poisoning and lead to a decreased degradation efficiency.[152] Although the direct anodic oxidation generally result in very poor degradation performance,[153] there are a few studies that report favorable HOPs abatement results.[154, 155]

The indirect oxidation process is based on the reactive species (e.g., •OH, H_2O_2, O_3, •Cl, Cl_2, ClO^-, $SO_4^{\bullet-}$, $S_2O_8^{2-}$) that produced on the surface of anodes. Among these reactive species, •OH is almost a defining requirement of the indirect oxidation process for its high redox potential (2.80 V/SHE). In most circumstances, indirect electrooxidation degradation of HOPs can be explained with •OH. However, the degradation pathway depends heavily on the adsorption status of •OH on anode surfaces. On one hand, the chemisorbed •OH on active anodes (e.g., Pt, RuO_2, IrO_2) can react drastically with anodes and form higher oxides or superoxides. This strong interaction between anodes and •OH decreases the catalytic efficiency of reactive species and lead to the partial transformation of HOPs, which called electrochemical conversion. On the other hand, the physisorbed •OH on inactive anodes (e.g., BDD, doped-SnO_2, PbO_2) presents a weak interaction with inactive anodes and can result in complete electrochemical degradation, which named electrochemical combustion. The classification of anodes mainly depends on the •OH production capacity, but not all electrodes can be clearly divided into the mentioned two types and some anodes manifest characteristics of both types.[108] To present the mentioned degradation process more intuitively, schemes based on the model proposed by Comninellis[156] are displayed in Fig.5.

View Article Online
DOI: 10.1039/C9EN00411D

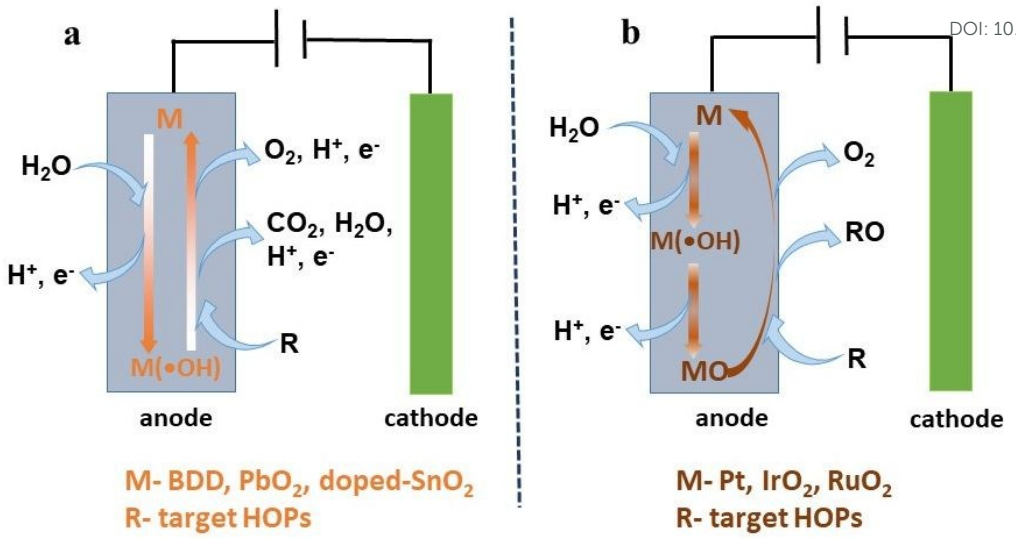

Fig.5 Mechanistic scheme of oxidative degradation of HOPs on inactive anodes (a) and on active anodes (b).

Other radicals such as chlorine- and sulfur-based species also play important roles in the mineralization of HOPs. Active chlorine species generated from solution begins with the direct oxidation of chloride ions on anode surface via Eq. (1), and the generated chlorine diffuses away from the electrode surface and yields Cl^- and HClO through disproportionation (Eq. (2)).

$$2Cl^- \rightarrow Cl_{2(aq)} + 2e^- \quad (1)$$

$$Cl_{2(aq)} + H_2O \rightarrow HClO + Cl^- + H^+ \quad (2)$$

The HClO in acid-base is in equilibrium with ClO^- with pK_a of 7.55 (Eq. (3)).[157]

$$HClO \leftrightarrow ClO^- + H^+ \quad (3)$$

It should be pointed out that the existence of these oxidative species highly depends on pH value (pH< 3, Cl_2; pH= 3-8, HClO; pH> 8, ClO^-). As a result, the oxidation of pollutants is more efficient in acidic media as the standard redox potentials of HClO (1.49 V/SHE) and Cl_2 (1.36 V/SHE) are higher than that of ClO^- (0.89 V/SHE).[133] Furthermore, the conversion of HClO to ClO_3^- (Eq. (4)) can interfere the degradation performance as ClO_3^- is less active in the oxidation reaction.[158]

$$6HClO + 3H_2O \rightarrow 2ClO_3^- + 4Cl^- + 12H^+ + 1.5O_2 + 6e^- \quad (4)$$

Likewise, chloride species can react with radicals and form perchlorates by Eqs. (5)- (8).

$$Cl^- + \bullet OH \rightarrow ClO^- + H^+ + e^- \quad (5)$$

$$ClO^- + \bullet OH \rightarrow ClO_2^- + H^+ + e^- \quad (6)$$

$$ClO_2^- + \bullet OH \rightarrow ClO_3^- + H^+ + e^- \quad (7)$$

$$ClO_3^- + \bullet OH \rightarrow ClO_4^- + H^+ + e^- \quad (8)$$

Actually, the evolution of ClO_4^- is an undesirable access because of its low oxidation capacity and serious hazardousness for human health.[133] Furthermore, those organo-chlorinated species formed are also detrimental to the mineralization process for their strong persistence and high toxicity.[108]

$S_2O_8^{2-}$ with a high redox potential (2.01 V/SHE) is another often mentioned radical because Na_2SO_4 is the most widely used electrolyte. The generation of $S_2O_8^{2-}$ is presented with Eq. (9).[159] This radical has a strong oxidation potential and can react with organic pollutants, which results in a desirable degradation. Interestingly, the potential of persulfate can be greatly enhanced with different activation methods,[160] and the related studies are reviewed by Matzek and Carter.[161] The $SO_4^{\bullet-}$ is another sulfur-based radical, which also shows a high redox potential (2.5-3.1V/SHE). The formation and transformation of sulfate radicals are presented as Eqs.(10)- (12).[160] Previous reports indicated that both persulfate radicals and sulfate radicals could facilitate the mineralization of organic pollutants due to their high oxidation ability.[160, 162, 163]

$$2SO_4^{2-} \rightarrow S_2O_8^{2-} + 2e^- \quad (9)$$

$$SO_4^{2-} \rightarrow SO_4^{\bullet-} + e^- \quad (10)$$

$$SO_4^{\bullet-} + H_2O \rightarrow SO_4^{2-} + \bullet OH + H^+ \quad (11)$$

$$S_2O_8^{2-} + e^- \rightarrow SO_4^{2-} + SO_4^{\bullet-} \quad (12)$$

Other radicals (e.g., H_2O_2 and O_3) are also quite important complements to •OH in the EOP process. More information can be found in the previous reviews.[133, 164]

It is necessary to place emphasis on the mineralization pathway of perfluorinated compounds (PFCs), due to the high persistence of C-F and the terrible toxicity of PFCs. In addition, it is suggested that the mineralization of PFCs cannot be solely explained by radicals (e.g., •OH), which is quite different from the degradation process of normal HOPs. Niu et al.[165] found that the degradation of PFCAs began with a direct anodic oxidation process (Eq. (13)), and the formed radicals (e.g., C_nF_{2n+1}•) can react with •OH or other radicals. With a series of reactions (intramolecular rearrangement and hydrolysis), PFCAs can be totally mineralized by repeating the CF_2-unzipping cycle, and the related reaction is presented in Eqs. (14)-(17). However, Li and co-authors suggested that the mineralization of PFOA (e.g., $C_7F_{15}COOH$) was primarily driven by •OH radicals (Eq. (18)) in an MW-Fenton-like process.[166] Indeed, mechanisms related to different PFCs and different degradation systems may vary significantly. More detailed information can be referred to previous review works,[28, 167] and a classical PFCs degradation process is presented in Fig. 6.[28]

$$C_nF_{2n+1}COO^- \rightarrow C_nF_{2n+1}COO\bullet + e^- \quad (13)$$

$$C_nF_{2n+1}COO\bullet \rightarrow C_nF_{2n+1}\bullet + CO_2 \quad (14)$$

$$C_nF_{2n+1}\bullet + HO\bullet \rightarrow C_nF_{2n+1}OH \quad (15)$$

$$C_nF_{2n+1}OH \rightarrow C_nF_{2n-1}OF + HF \quad (16)$$

$$C_nF_{2n-1}OF + H_2O \rightarrow C_{n-1}F_{2n-2}COO^- + HF + H^+ \quad (17)$$

$$C_7F_{15}COO^- + HO\bullet \rightarrow C_7F_{15}COO\bullet + OH^- \quad (18)$$

Therefore, due to the complexity of HOPs structure, radical species, and water matrix, the oxidation degradation pathway should be explored on a case-by-case basis with the assistance of advanced analysis methods.

View Article Online
DOI: 10.1039/C9EN00411D

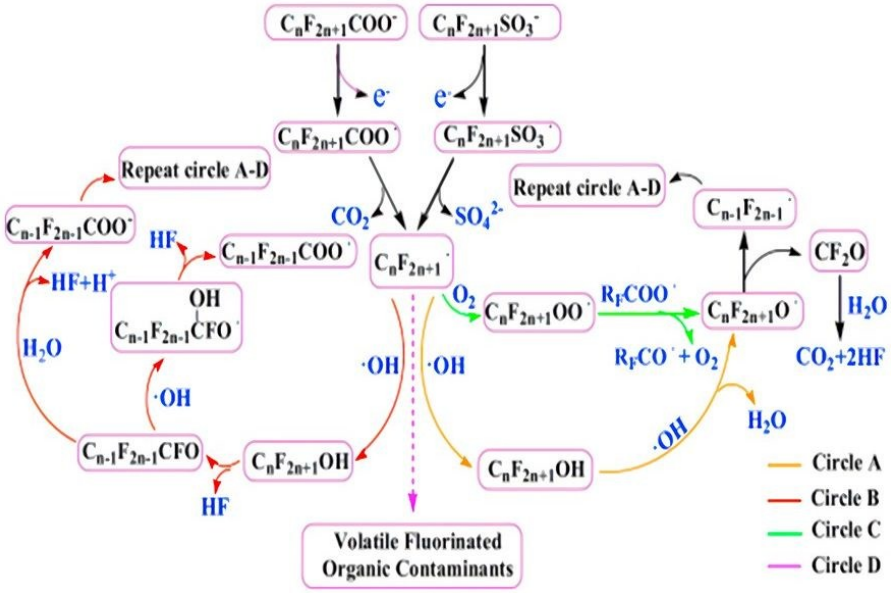

Fig.6 Schematic diagram illustrating the electrochemical oxidation mechanism of PFCs. Reproduced with permission from ref. 28, Copyright 2016, Elsevier.

3. Catalysts for electroreductive dehalogenation

The electrocatalytic reduction is a highly effective method for the degradation of HOPs. Different from the electrooxidation process that generally results in complete mineralization of HOPs, the overall goal of the electroreductive process is either total dehalogenation (principally hydrodehalogenation) of HOPs to ease the further treatment, or the transformation into value-added chemicals.[30, 168] In this part of the review, commonly reported catalysts such as Ag-based electrodes, Pd-based electrodes, and metal complexes (organometallic compounds) are analysed. Subsequently, diverse reduction mechanisms are reviewed to provide a better insight into the electrolytic scission of C-X bonds.

3.1. Ag-based catalysts

Recently, silver-based cathodes have attracted much attention owing to their strong electrocatalytic activities toward dehalogenation of HOPs. The high affinity of Ag for halide ions plays the vital role.[169, 170] Compared with the classic glass carbon electrode which commonly acts as a noncatalytic cathode, the electrochemical breakage of C-X bonds at

View Article Online
DOI: 10.1039/C9EN00411D

silver cathode occurs at a much less negative potential.[171] Several critical examples involve the ERD process with Ag-based cathodes are summarised in Table 5.

Table 5 Summary of representative HOPs electroreductive dehalogenation using Ag-based cathodes.

electrode	electrolyte	HOPs	Main Products/ Results	Ref.
Ag ($0.071\ cm^2$)	DMF① + 0.05 M TMAP②	2-bromo-5-chlorothiophene (**1**) 3-bromo-2-chlorothiophene (**2**) 2,5-dibromothiophene (**3**)	2-Chlorothiophene (**1**) 2-Chlorothiophene (**2**) 2-bromothiophene (**3**)	171
Etched Ag-PVP-Ni	0.05 M NaOH	50 ppm Alachlor™	Conversion rate 93 ± 3%; deschloroalachlor 69 ± 4%; Cl^- 77 ± 2%	169
Ag-ZSM-5/SS	0.1 M TEAP-MeCN	2.6 mM $PhCH_2Cl$	yield of electrocarboxylation 61%	172
Ag ($0.071\ cm^2$)	DMF + 0.050 M $TBABF_4$③	10 mM 1-bromo-6-chlorohexane (**1**) 10 mM 1-chloro-6-iodohexane (**2**)	1-chlorohexane 63%, n-hexane 18% 6-chloro-1-hexene 10% (**1**); 1-chlorohexane 43%, 6-chloro-1-hexene 23%, 1,12-dichlorododecane 22% (**2**)	173
roughened Ag	0.5 M $NaClO_4$ (anolyte)+0.5 M $NaClO_4$ (catolyte)	5 mM 3,4,5,6-Tetrachloropicolinic Acid(TeCP) (pH = 7.0)	3,5,6-T 83.1%, TeCP 8.4%, 3,6-D 4.3%	174
roughened Ag	0.5 M $HClO_4$ (anolyte)+0.5 M $NaClO_4$ (catholyte)	5 mM TeCP (pH = 4.0)	TeCP 60.0%, 3,5,6-T 35.0%, 3,5-D 4.3%	174
roughened Ag mesh	0.5 M NaOH	3.33 mM 3,5,6-trichloropicolinic acid (3,5,6-T)	3,5,6-T 61%, 3,6-D 38%, 3,5-D 4.3%	175
Ag	DMF + 0.05 M TMAP	5 mM 1,2-dibromohexane (**1**) 10 mM 1,6-dibromohexane (**2**)	1-hexene 107% (**1**); 1-hexene 22%, n-hexane 39%, 1,5-hexadiene 18%, 5-hexen-1-ol 7% (**2**)	176

① dimethylformamide; ② tetramethylammonium perchlorate; ③ tetra-n-butylammonium tetrafluoroborate

Nanosizing is an effective strategy to enhance the performance of Ag cathodes as well as to reduce the consumption of this precious metal.[172, 177] Ag nanoparticles present distinctive capabilities that are different from the bulk material because of their decreased dimensions and improved surface to volume ratios.[178] For instance, Sui and co-workers[172] fabricated an Ag-ZSM-5/SS zeolite modified electrode with a facile one-step method, and Ag nanoparticles (average diameter of 9 nm) was formed in-situ with ZSM-5 films grown on the stainless steel. The addition of well-dispersed Ag nanoparticles highly elevated the conductivity of the zeolite film, with a low resistance of 4 $m\Omega \bullet sq^{-1}$. Further study suggested that the electrochemically active surface areas played a key role in determining the catalytic performance. Compared to the Ag bulk electrode, ZSM-5 provided more sites for dispersing and stabilizing Ag nanoparticles and promoted Ag nanoparticles' catalytic activity. As a result, The Ag-ZSM-5/SS displayed marvelous electrocatalytic activities towards electrocarboxylation of $PhCH_2Cl$, with the electrocarboxylation yield of 61% was obtained at

-1.1 V. However, the application of Ag bulk electrode showed a lower yield of 40% at a more negative potential of -1.5 V. Brzózka et al.[178] systematically designed three Ag electrodes, namely, silver nanohemisphere (Ag-NHS) electrode, nanowire (Ag-NW) array electrode and silver rod (Ag-bulk) electrode, and the detailed synthesis routes of Ag-NHS electrode and Ag-NW electrode are presented in Fig. 7 a. The as-prepared two nanomaterials exhibited quite different morphologies and diameters. Ag-NHSs possessed an average diameter of 126nm and height of 126nm, while the diameter and length of Ag-NWs were 90nm and 3.5 μm (Fig. 7 b-d). The smaller size of Ag-NWs could provide more active sites for the electrochemical reaction. Compared with Ag-bulk electrode, both Ag-NHS and Ag-NW manifested better electrochemical performance and stability in the degradation of $CHCl_3$. Furthermore, the Ag-NW showed about 200 mV less over potential than Ag-bulk electrode, and that of Ag-NHS was about 100 mV.

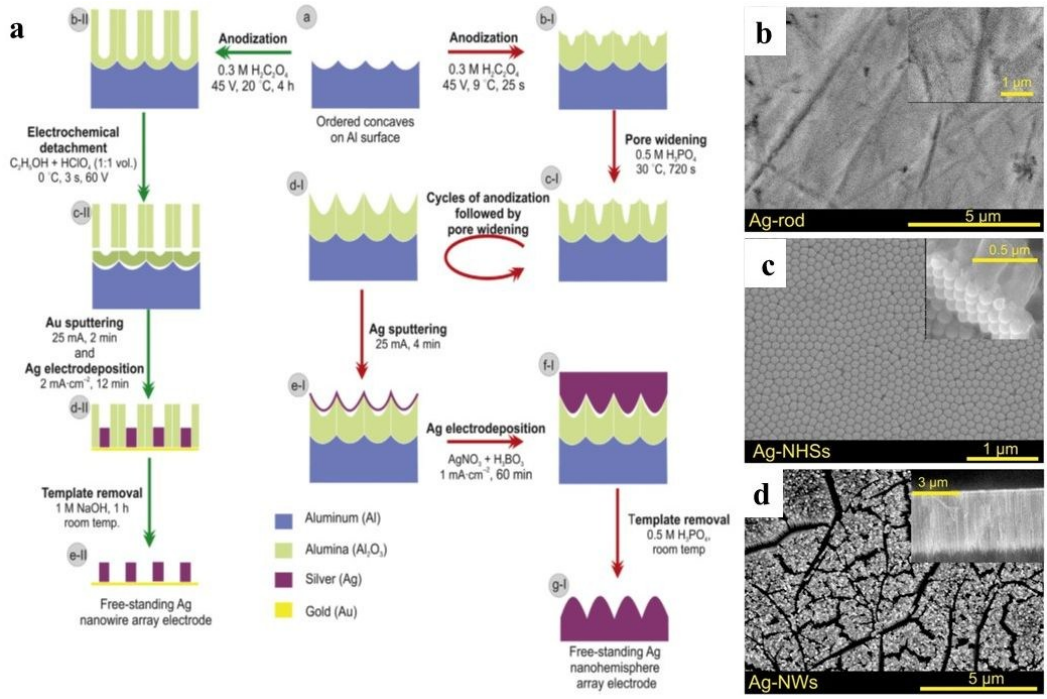

Fig.7 Schematic representation of synthesis of the free-standing Ag nanohemisphere and Ag nanowire array electrodes (a); Top-view SEM images of Ag electrodes: Ag rod (Ag-bulk) after mechanical polishing (b); Ag nanohemisphere array electrode (Ag-NHSs) after

silver electrodeposition (c); Ag nanowire array electrode (Ag-NWs) after silver electrodeposition (d). Reproduced with permission from ref. 178, Copyright 2017, Elsevier.

Another encouraging way to boost the electrocatalytic activity of Ag cathodes is based on changing Ag bulk to multi-metallic electrodes.[179, 180] Vanrenterghem et al.[179] prepared bimetallic Ag-Ni glassy carbon supported cathodes (Ag-Ni/GC) with a two-step procedure, and the designed Ag-Ni/GC electrodes were compared with Ag/Ni foam electrodes for the reduction of benzyl bromide. Their results suggested that pretreatment such as cathodising in alkali and scanning in acid had an obvious effect on the surface composition of Ag-Ni/GC cathodes, with the cathodising and scanning processes leading to a higher atomic ratio of Ag-Ni as 1/13 and 1/4 respectively in comparison with the 1/17 for the non-treated one. Further study indicated that Ag-Ni/GC electrode cathodised in alkali was the best one for the degradation of benzyl bromide, and the yield of the sole product toluene (49 mol%) was higher than that of bulk Ag cathode (37 mol%). Hence, the presence of Ni has a beneficial influence on the electrocatalytic capacity of Ag.

Table 5 also suggests that the degradation performance of Ag-based cathodes relies heavily on HOP structures, apart from the intrinsic properties of electrodes. In particular, the molecular structures of HOPs have a significant impact on the dissociative electron transfer (DET) process in the dehalogenation reaction. For example, electroreduction of a series of aliphatic and aromatic bromides on the silver cathode has been studied by cyclic voltammetry in 1-butyl-3-methylimidazolium tetrafluoroborate ([BMIm]BF_4).[170] In the case of aromatic bromides, the electron transfer process supplies a radical anion intermediate that further dissociates to R• and Br^-, and this reaction called a stepwise mechanism. It is worth noting that the electrocatalytic activity for aromatic bromides relies highly on the molecular structure of RBr, decreasing with growing ability of the RBr to delocalize the negative charge in the radical anion intermediate. However, for the reduction of different aliphatic bromides,

Ag always displays a great electrocatalytic activity, which has been confirmed by several studies.[181-183]

3.2. Pd-based catalysts

Noble metal catalysts (e.g., Pd, Ru, Rh, Pt) that show great electrocatalytic activities have also been applied to the electrochemical dehalogenation of HOPs. Among these, Pd is the most frequently used cathode as it possesses an extraordinary ability to intercalate hydrogen within its lattice.[184] Moreover, the formed active chemical species Pd-H normally acts as the source of atomic hydrogen (H*).[1, 185] Quite different from the dissociative electron transfer (DET) process with Ag-based catalysts, electrocatalytic hydrodehalogenation (ECH) process using atomic hydrogen is the main HOPs degradation pathway with Pd-based electrodes. Therefore, enormous efforts have been devoted to the development of high-performance Pd-based cathodes that can produce sufficient H* and have a long lifetime. A summary of representative HOPs electroreductive dehalogenation studies with Pd-based cathodes is presented in Table 6.

Table 6 Summary of representative HOPs electroreductive dehalogenation using Pd-based cathodes in recent years.

Cathode	Preparation methods	HOPs	C_{HOP} / mg L^{-1}	Electrolyte	Other parameters	HOP Removal rate/%	Ref.
TiC-Pd/Ni	electroless deposition	2,4-dichlorobenzoic acid	0.2 mM	10 mM Na_2SO_4	10 mA; 80 mL (catholyte), 40 mL (anolyte); pH 4; 298 ± 0.3 K	99.8 (90min)	18
Pd/PANI/Ni	two-step galvanostatic electropolymerization method	2,4-dichlorophenol	0.5 mM	0.05 M Na_2SO_4	5 mA; 50 mL(catholyte), 50 mL (anolyte); 40 °C	89.1 (120min)	186
Pd/MnO_2/Ni	electrodeposition	2,4-dichlorobenzoic acid	0.2 mM	10 mM Na_2SO_4	10 mA; 80 mL (catholyte), 40 mL (anolyte); 30 ± 1 °C; pH 4	100 (120min)	187
Pd/CNTs	impregnation method	4-chlorophenol	-	-	H_2 10 mL min^{-1}; 313 K	90 (50min)	188
Pd/PANI-NiHCF-CNT/Ti	electrodeposition	4-chlorophenol	100	0.1 M Na_2SO_4	1 mA cm^{-2}; 100 mL (catholyte), 100 mL (anolyte); 16cm^2	98.59 (120min)	189
EDPd/CNx/Ni	electrodeposition	3,6-dichloropicolinic acid	0.226 mM	34.2 mM NaCl	2.5 mA cm^{-2}; 25 °C; 72 mL (catholyte), 36 mL (anolyte)	97.8(4h)	190
Ni/Pd	electrodeposition	Para-	25	50 mM	10 mA cm^{-2}; pH	99	191

		chloronitrobenzene		Na_2SO_4	7; 25 °C; 50 mL	(30min)	
Pd/CNTs-nafion film/Ti	dip-coating method; electroplating	2,3,5-trichlorophenol	100	0.05 M Na_2SO_4	5 mA; pH 2.3; 25 °C; 50 mL (catholyte), 50 mL (anolyte)	100 (100min)	192
PE-Pd/Ni	pulsed electrodeposition	2,4-dichlorophenoxyacetic acid	0.226 mM	34.2 mM NaCl	1.5 mA cm^{-2}; 25 °C; 72 mL (catholyte), 36 mL (anolyte)	98 (3h)	193
1Rh-0.5Pd/Ni	electrodeposition	4-fluorophenol	0.1 mM	0.1 M H_2SO_4 (anolyte); 20 mM aqueous phosphate buffer(catholyte)	H_2 10 mL min^{-1}; 30 °C; 40 mL (catholyte), 40 mL (anolyte); pH 3	100 (45min)	194
Pd–Fe/graphene	photo-induced reduction	4-bromophenol	100	0.03 M Na_2SO_4	150 mL; 16 cm^2; 25 mA cm^{-2}; pH 7	100 (60min)	195
$Pd_{58}Ni_{42}$(SDBS)/PPy/Ti	electrodeposition	pentachlorophenol	10	0.05 M Na_2SO_4	5 mA; pH 2	100 (90min)	196
Pd-In/Al_2O_3	coprecipitation	trichloroacetic acid	0.5	2 mM Na_2SO_4	50 mL (catholyte), 50 mL (anolyte); 0.9 mA cm^{-2}; pH 7	94 (30min)	197

The nature of Pd cathode materials plays a critical role in the dehalogenation process, as well as some key parameters, including fabrication methods, interlayers, and substrates. Among these, the fabrication methods and interlayers are emphasized in this work, as well as the coupling strategy. The fabrication method plays a vital role in determining the catalytic performance of electrodes. He and co-workers[193] fabricated Pd-based electrodes by pulsed electrodeposition (PE-Pd/foam-Ni) and traditional chemical deposition (CD-Pd/foam-Ni). Compared with the latter one, PE-Pd/foam-Ni possesses upgraded dechlorination efficiency and current efficiency for the degradation of 2,4-dichlorophenoxyacetic acid (2, 4-D). The reason was that PE-Pd/foam-Ni possessed a smaller particle size, a higher percentage of exposed (111) facets together with a higher number of edge/ corner sites than that of CD-Pd/foam-Ni. These characteristics favored the production and stabilization of chemisorbed H*. Furthermore, to exploit the most intrinsic properties of Pd catalysts, a robust interlayer with a high specific surface area is often required.[189, 190] For instance, Li et al.[186] found that the conductive polymer polyaniline (PANI) in the Pd/PANI/Ni electrode existed in the form of needle-shaped, and Pd^0 clusters dispersed quite well in the network on PANI. The Pd/PANI/Ni electrode owned a higher specific surface area (6.8 m^2g^{-1}) than Pd/Ni electrode, which resulted in a better removal efficiency for 2,4-dichlorophenol than the latter one (89.1% vs. 71.1%). Moreover, Luo and coworkers[187] examined the role of MnO_2 in a Pd/MnO_2/Ni

foam electrode, and they found that the introduction of MnO_2 could drastically decrease the consumption of Pd by four times when achieved complete removal of 2,4-dichlorobenzoic acid (Fig. 8 a). Surprisingly, MnO_2 could promote the water dissociation and provide more atomic H* for dechlorination, which is the main reason for the electrochemical dehalogenation improvement of Pd/MnO_2/Ni foam electrode (Fig. 8 b). Coupling with other metal(s) is another way to decrease the dosage of Pd and boost its electrocatalytic properties. The synergistic effect of metals can upgrade the activity and selectivity of catalysts and relieve catalyst aging and loss.[197, 198] For example, Wu and co-workers[198] developed a palladium-nickel/multi-walled carbon nanotubes/graphite felt electrode (Pd-Ni/MWCNTs/GF) for the electrocatalytic hydrodechlorination of 4-chlorophenol (4-CP). Experimental results suggested that the interaction between Pd and Ni was beneficial for Pd reinforcement, and thus improving the stability of electrodes. Compared to those cathodes with single-metal Pd, Pd-Ni/ MWCNTs/GF demonstrated better stability and higher reactivity for the degradation process, with complete removal of 4-CP being achieved in 30 min.

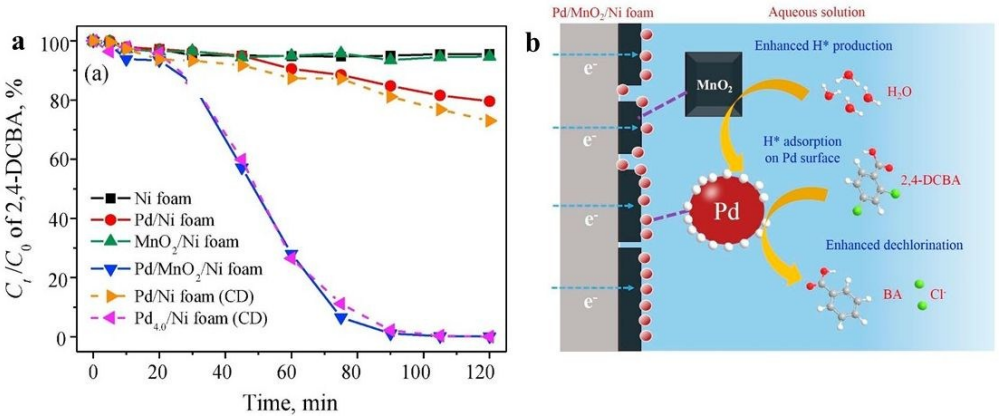

Fig.8 The removal efficiency of 2,4-DCBA by six different electrodes (a); schematic of 2,4-DCBA dechlorination process by the Pd/MnO_2/Ni foam electrode (b). Reproduced with permission from ref. 187, Copyright 2018, Elsevier.

Experimental parameters (e.g., pH value, applied current, electrolyte) also impact the performance of cathodes heavily.[185, 198, 199] Take the cathode potential as an example, Jiang et

View Article Online
DOI: 10.1039/C9EN00411D

al.[199] found that the applied potential had a great influence on the evolution of three different hydrogen species, namely adsorbed atomic hydrogen (H^*_{ads}), absorbed atomic hydrogen (H^*_{abs}), and molecular hydrogen (H_2). Combined with the degradation efficiency and kinetics of 2,4-Dichlorophenol (Fig. 9), they confirmed that H^*_{ads} is the active species, H^*_{abs} is inert, while H_2 bubbles are detrimental to the electrocatalytic hydrodechlorination reaction. Consequently, to achieve a desired degradation result, a moderate potential is needed to produce sufficient H^*_{ads} and limit the negative effect of H_2.

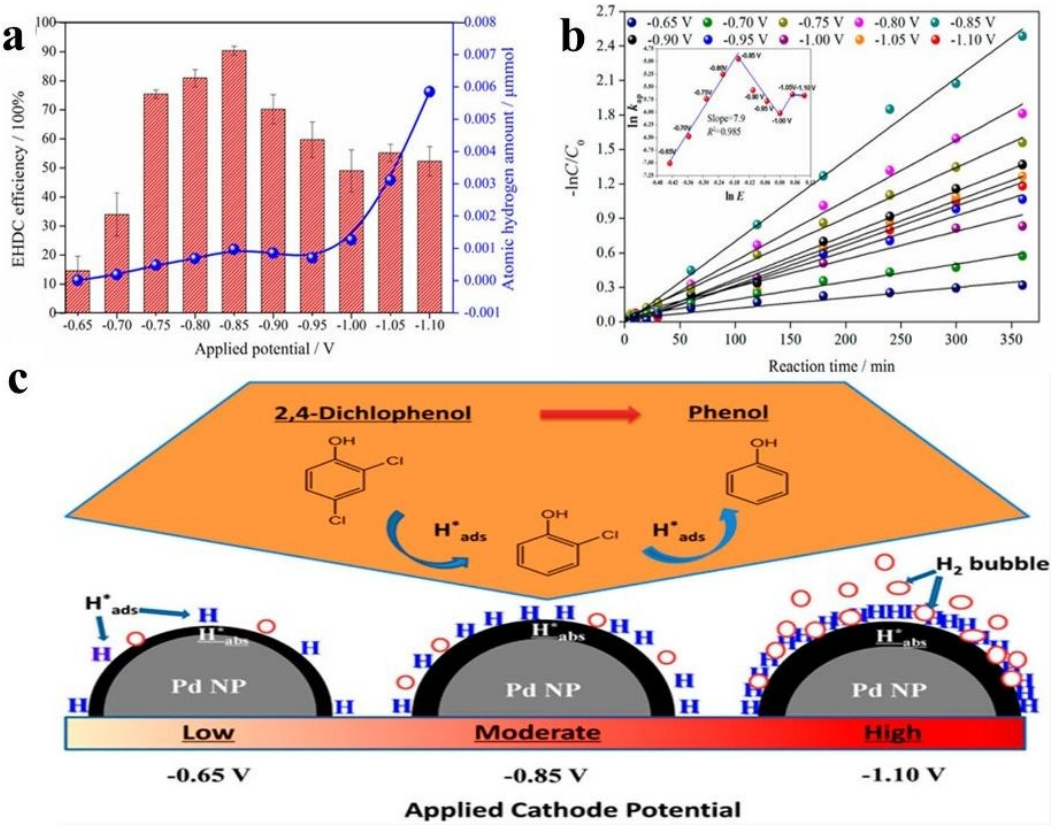

Fig.9 The correlation of EHDC efficiency (denoted as $(C-C_0)/C_0 \times 100\%$) and H^*_{ads} evolution on C-Pd under different cathode potentials from -0.65 to -1.10 V (a); pseudo-first-order representation of the EHDC reaction of 2,4-DCP versus time under different cathode potentials (The inset is the relationship between ln k_{ap} and ln E.) (b); schematic illustration of the potential-dependent 2,4-DCP EHDC mechanism (c). Reproduced with permission from ref. 199, Copyright 2015, American Chemical Society.

View Article Online
DOI: 10.1039/C9EN00411D

3.3. Metal complex-based catalysts

In recent years, electrogenerated low-valent metal complexes, known as mediator catalysts, have attracted immense attention to the catalytic reduction of HOPs. These metal complexes are generated at a more positive potential than that needed for the direct breakage of C-X bonds. Surprisingly, these electrogenerated catalysts possess great catalytic activities, preparative accessibility, as well as structural flexibility.[2, 200] To date, nickel together with cobalt species are the most prominent catalysts for the reduction of HOPs, and Table 7 summarises the catalytic performance of the representative metal complexes.

Nickel(I) salen, usually electrogenerated at glass carbon cathodes in either acetonitrile or dimethylformamide, has presented an excellent catalytic activity towards the reduction of different HOPs, including 1,6-dihalohexanes, 1-bromodecane, 1-iododecane, α,ω-dihaloalkanes, 6-bromo-1-hexene, haloalkynes, cyclohexyl bromide, and cyclohexyl iodide, etc.[201, 202] For example, Wagoner and co-workers[203] examined the catalytic reduction of 1,2,5,6,9,10-hexabromocyclododecane (HBCD) with nickel(I) salen in dimethylformamide. The bulk electrolysis of less than 20.0 mM HBCD underwent in a six-electron process, which resulted in the conversion of the initial pollutant to 1,5,9-cyclododecatriene (88-95%), with small amounts of cyclododeca-1, 5-dien-9-yne (3-4%). In addition, it is worth noting that nickel (I) salen-catalyzed reduction of alkyl halides often leads to alkylation of one or both imino (C=N) bonds, which seriously impedes the dehalogenation process.[2, 202] Under such circumstance, structurally modified nickel(I) salen species have exhibited a better performance, mainly due to they possess methyl protecting group on imino (C=N) bonds.[201, 204]

Cobalt complexes such as cobalt(I) alamin (vitamin B_{12}), cobalt(I) salen, cobalt(I) polypyridyl, and cobalt (I) phthalocyanine complexes have displayed great catalytic

View Article Online
DOI: 10.1039/C9EN00411D

performance toward the reduction of organohalides.[2, 30] Among these complexes, vitamin B_{12} that consists of a cobalt atom coordinated by four nitrogen atoms of the corrin ring. Its derivatives has been widely investigated for its extensive application in synthesis, bioremediation, biocatalysis, as well as electrocatalysis, especially in the electrocatalytic reduction process of organic halides.[205-207] As reported, vitamin B_{12} species are able to reduce arenes, ethanes, ethylenes, higher alkanes, chlorinated methanes, etc.[30, 206, 207] More in-depth information related to the vitamin B_{12} dehalogenation performance can be referred to a recent review.[206] Similar to nickel(I) salen, cobalt(I) salen is another extensively discussed catalyst in the scission of C-X bonds. In a typical study, 1,1,1-trichloro-2,2,2-trifluoroethane (CFC-113a) was reduced by electrogenerated cobalt(I) salen at a glassy carbon cathode. Surprisingly, CFC-113a (10.0 mM) has been successfully converted, with the main product distribution of 2,2-dichloro-1,1,1-trifluoroethane (52%), 2-chloro-1,1,1-trifluoroethane and 2-chloro-1,1-difluoroethene (7%), and 1,1-difluoroethene (1%). In addition, the salen ligand of cobalt(I) salen was modified through the addition of a CF_3CCl_2- or CF_3CHCl- moiety to the C=N bond in the catalytic reduction process.[208]

Table 7 Summary of representative HOPs electroreductive dehalogenation using metal complex cathodes.

Metal complex	electrolyte	HOPs	Main Products	Ref.
1.0 mM nickel(I) salen	DMF + 0.1 M $TBABF_4$	10.0 mM 1,2,5,6,9,10-hexabromocyclododecane	isomers of 1,5,9-cyclododecatriene (95%), isomers of cyclododeca-1,5-dien-9-yne (3%)	203
2.0 mM nickel(I) salen	DMF + 0.1 M $TBABF_4$	2.0 mM cyclohexyl bromide (**1**) 2.0 mM cyclohexyl iodide (**2**)	Cyclohexane (61%), cyclohexene (40%), bicyclohexyl (5%) (**1**); Cyclohexane (65%), cyclohexene (15%), bicyclohexyl (7%) (**2**)	202
2.0 mM cobalt(I) salen	DMF + 0.1 M $TBABF_4$	2.0 mM cyclohexyl iodide	Cyclohexane (63%), cyclohexene (22%), bicyclohexyl (12%)	202
2.0 mM Cobalt(I) Salen	DMF + 0.1 M $TBABF_4$	0.202 mM 1,1,1-Trichloro-2,2,2-trifluoroethane	2,2-dichloro-1,1,1-trifluoroethane (52%), 2-chloro-1,1,1-trifluoroethane + 2-chloro-1,1-difluoroethene (7%), 1,1-difluoroethene (1%)	208
1.0 mM structurally modified nickel(I) salen	DMF + 0.1 M $TBABF_4$	10.0 mM 1-bromodecane (**1**) 10.0 mM 1-iododecane (**2**)	n-eicosane (70%), n-decane (8%), 1-decene (4%), N,N-dimethylundecanamide (4%) (**1**); n-eicosane (63%), n-decane (12%), 1-decene (3%), N,N-dimethylundecanamide (5%) (**2**)	201
2.0 mM Ni(II) Salen	DMF + 0.05 M $TBABF_4$	20 mM benzyl bromide (**1**) 20 mM 1-bromomethylnaphthalene (**2**)	toluene (48%), toluene (19%), benzyl ether (18%) (**1**); 1-methylnaphthalene (52%), 1,2-bis(1-naphthyl)ethane (30%), bis(1-naphthylmethyl) ether (**2**)	209
2.0 mM Ni(II) Salen	DMF + 0.05 M $TBABF_4$	5.0 mM 4,4'-(2,2-dichloroethene-1,1-diyl)bis(chlorobenzene)	1,1-Diphenylethene (14%), 1-Chloro-4-(1-phenylvinyl)benzene (51%)	210
1.0 mM nickel(I) salen	DMF + 0.1 M $TBABF_4$	10.0 mM 1-Iodooctane (**1**); 10.0 mM 1-Bromooctane (**2**); 5.0 mM 1-Bromo-5-decyne	Octane (4%), 1-octene (9%), hexadecane (87%) (**1**); Octane (5%), 1-octene (4%), hexadecane	211

	(**3**); 5.0 mM 1-Iodo-5-decyne (**4**);	(89%) (**2**); Dec-5-yne (11%), dec-1-en-5-yne (3%), pentylidenecyclopentane (74%) (**3**); Dec-5-yne (8%), dec-1-en-5-yne (3%), pentylidenecyclopentane (88%) (**4**)

3.4. Electroreductive dehalogenation mechanisms

Mechanisms of the electroreductive scission of C-X bonds have been broadly investigated, and still are, discussed in many authoritative studies,[1, 2, 168] and are also outlined in this work briefly.

Firstly, the heterogeneous and homogeneous electron transfer (ET) plays an important role in the reduction process.[168] The extensively researched dissociative electron transfer (DET) theory can account for vast experimental results when Ag-based cathodes are applied, and a scheme mechanism of DET is provided in Fig. 10 a.[212] The scheme **a** is a stepwise mechanism, involving the formation of an intermediate radical anion ($RX^{\bullet -}$) before the cleavage of the C-X bond, while scheme **b** that named concerted mechanism represents the simultaneous electron transfer and the C-X bond breaking. Literature data suggest that degradation of aromatic halides mainly follows the stepwise mechanism, whereas aliphatic halides prefer the concerted one,[1, 170] but there are several exceptions to this rule.[212] Hence, it is necessary to carry out careful exploration of the reaction system before assigning one or another mechanism to a typical degradation process. Additionally, the scheme **c** that is a variant of the concerted mechanism referred as sticky DET, and two fragments (e.g., $R^{\bullet}$ and X^-) can induce ion-dipole interactions in the solvent cage before they diffuse apart in this procedure. Generally, many subsequent reactions will occur and produce dimers and hydrodehalogenated species (Eqs. (19)- (23)), and SH is the solvent.[2, 168]

$$R^{\bullet} + e^- \rightarrow R^- \quad (19)$$

$$R^{\bullet} + SH \rightarrow RH + S^{\bullet} \quad (20)$$

$$R^- + SH \rightarrow RH + S^- \quad (21)$$

View Article Online
DOI: 10.1039/C9EN00411D

$$R^- + RX \rightarrow R\text{-}R + X^- \quad (22)$$

$$R^\bullet + R^\bullet \rightarrow R\text{-}R \quad (23)$$

Secondly, when electrogenerated low-valent metal complexes are employed as catalysts, the ET process will occur in homogeneous conditions.[168] In a representative work, Chan and co-workers [213] discussed the use of cobalt porphyrin to catalyze the hydrodehalogenation of aryl bromides, and the plausible mechanism is illustrated in Fig. 10 b. Initially, Co^{II}(ttp) abstracts a bromine atom from ArBr to generate Co^{III}(ttp)Br and Ar•. Then, the Ar• abstracts an H from solvent to form the ArH, while the Co^{III}(ttp)Br undergoes ligand substitution with KOH and generates Co^{III}(ttp)OH and KBr. Afterwards, Co^{III}(ttp)OH produces H_2O_2 and regenerates Co^{II}(ttp) by reductive elimination. Subsequently, the H_2O_2 catalyzed by Co^{II}(ttp) or base to H_2O and O_2.

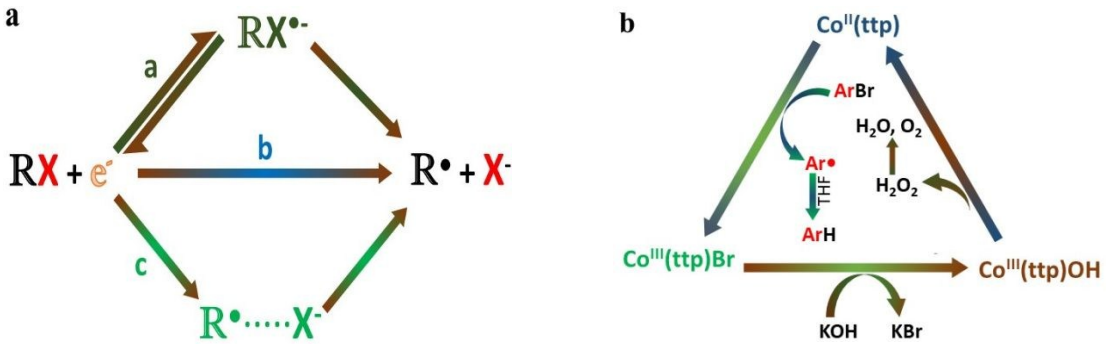

Fig.10 The general mechanism of dissociative electron transfer (a). Reproduced with permission from ref. 212, Copyright 2015, Royal Society of Chemistry. Proposed hydrodehalogenation mechanism of aryl bromides (b). Reproduced with permission. Reproduced with permission from ref. 213, Copyright 2015, Elsevier.

Finally, the indirect dehalogenation process with the H^*_{ads} is another efficient way to degrade HOPs,[168] and this mechanism often associates with the application of Pd-based catalysts. The reductive dehalogenation process is known as electrocatalytic hydrogenolysis (ECH),[214, 215] which can be described as chemisorbed hydrogen atoms first generated on the cathode

surface by electrolysis of water and then react with adsorbed HOPs. The key steps are listed in Eqs. (24)- (29).[193, 214, 216]

$$2H_2O\ (2H_3O^+) + 2e^- + 2M \rightarrow 2(H)_{ads}M + 2OH^-\ (2H_2O)\ \text{(Volmer step)} \quad (24)$$

$$R\text{-}X + M \rightarrow (R\text{-}X)_{ads}M \quad (25)$$

$$(R\text{-}X)_{ads}M + 2(H)_{ads}M \rightarrow (R\text{-}H)_{ads}M + 2M + HX \quad (26)$$

$$(R\text{-}H)_{ads}M \rightarrow R\text{-}H + M \quad (27)$$

$$(H)_{ads}M + H_2O + e^- \rightarrow H_2 + OH^- + M \quad \text{(Heyrovsky step)} \quad (28)$$

$$(H)_{ads}M + (H)_{ads}M \rightarrow H_2 + 2M \quad \text{(Tafel step)} \quad (29)$$

where M represents the metallic surface, and HX denotes HOPs. Actually, the ECH process is just a combination of Eqs. (21)- (24), whereas the hydrogen evolution reaction (HER) reaction (Eqs. (25)- (26)) occurs as the competition process. Hence, it is of great importance to depress the HER reaction in the degradation process.

The HER process starts with the formation of H^*_{ads} and then the electrochemical desorption (Volmer-Heyrovsky), or the recombination of the atomic H^*_{ads} (Volmer-Tafel).[217-219] Both HER and ECH process require abundant surface adsorbed hydrogen through the Volmer step, so the key to suppress the HER process is to block the Heyrovsky step or the Tafel step. Currently, two strategies are often applied to optimize the degradation process through effectively vanquish the HER process. The first strategy is using cathode materials with a favorable ability for the generation and retainment of H^*_{ads}. In this regard, Pd distinguishes itself not only for its high efficiency in taking up protons to generate H* but also due to its property to retain the H* by adsorption onto the Pd surface (H^*_{ads}) and absorption to the Pd atoms via the formation of Pd hydride (H^*_{abs}).[220] Therefore, Pd can maintain a high surface hydrogen concentration for the ECH process. In most of the cases, it is difficult for other materials (e.g., Pt, Rh) to retain the generated H^*_{ads}, since the H^*_{ads} are easily transform to molecular hydrogen through the Heyrovsky step or the Tafel step. Recently, several effective

methods have been applied to further enhance the selectivity of Pd.[190, 220] For example, Liu and co-workers[220] found that the defective sits in Pd nanowires could enhance the stability of the generated H^*_{ads} and suppress the HER process. Due to the magnificent H^*_{ads} generation/provision capacity, the defect-rich Pd nanowires exhibited a higher 2,4-dichlorophenol removal efficiency with a six-times-lower Pd loading than the unmodified Pd materials. Another strategy to extinguish the HER process is to optimize the operating parameters, such as the cathode potential,[185, 199, 221, 222] pH value,[223] and dissolved oxygen[217]. Among these factors, the cathode potential is most frequently studied. Commonly, the kinetics of H^*_{ads} production are modulated by the cathode potential, and a more negative potential will usually hasten H^*_{ads} generation, which could offer sufficient H^*_{ads} for enhanced ECH.[221] However, as a side reaction, H^*_{ads} may evolve into H_2 through the Heyrovsky step or the Tafel step at a more reductive potential. Such side reaction can compete with ECH in H^*_{ads} utilization, and the generated hydrogen bubbles also interfere with the mass transfer of H^+ and HOPs to the cathode surface, resulting in a decay in ECH efficiency.[199] As a result, an optimal cathode potential is critical for the restraint of HER.

However, it should be noted that there is still lacking of fundamental principles for interpreting the dehalogenation mechanism of a typical HOP without experimental examination due to that fact that there are many unexpected observations related to the mechanisms mentioned above.[187, 195, 197, 212, 215] For instance, Liu et al.[197] found that atomic H^*_{ads} formation function and the electron transfer process both existed in the trichloroacetic acid (TCAA) removal process, while the enhanced indirect atomic H^*_{ads} reduction process played a principal role in the degradation process (Fig. 11).

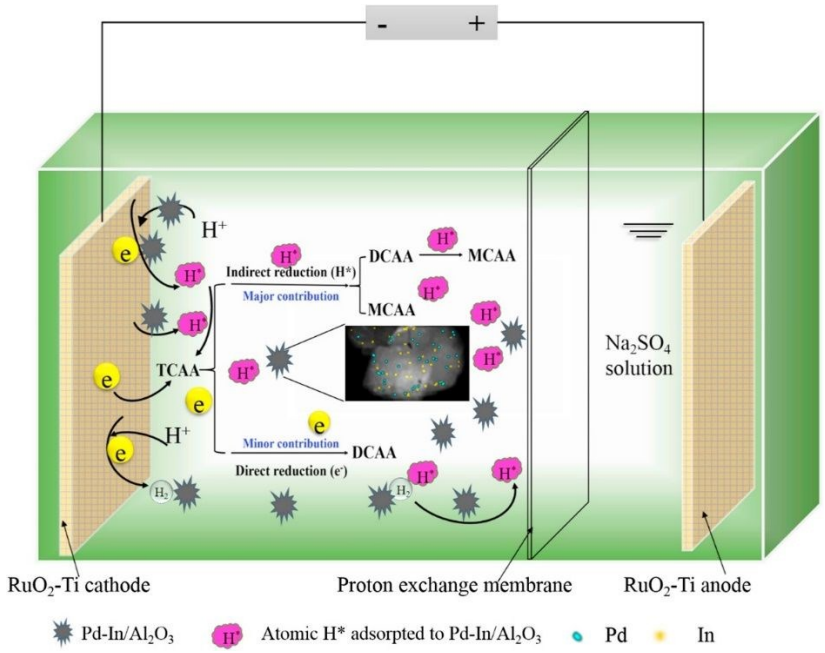

Fig.11 Schematic diagram of reaction mechanism for TCAA reduction over Pd-In/Al_2O_3. Reproduced with permission from ref. 197, Copyright 2017, Elsevier.

4. Integrated Technologies

Recently, the number of strategies has grown rapidly with the development of coupling synergistic processes based on the combination of electrocatalysis.[224] The coupling can upgrade the overall degradation performance toward HOPs due to the synergy between different sophisticated processes.[224, 225] Fenton reaction,[87, 226] membrane filtration,[227, 228] biological treatment,[225, 229] photocatalysis,[230, 231] ozonation,[225, 232] adsorption,[225, 233] ultrasound,[230, 234] UV irradiation,[230, 235] microwave,[236] and thermolysis[237, 238] are the widely reported methods that can assist the electrochemical activity of electrocatalysis. In this part of the review, the first four methods are detailed due to their wide applications. A list of representative HOPs dehalogenation with synergistic methods is shown in Table 8.

Table 8 Summary of representative HOPs dehalogenation using synergistic methods.

Method	Experimental conditions	HOPs	Degradation rate (%)	Ref.
Reactive electrochemical filter system	50 mM Na_2SO_4; inlet flow rate 1.8 L min^{-1}; 25 ± 1 °C; pH 7; 0.25A; 3.0V	50 mg L^{-1} rhodamine B	97.6(30min)	227
Reactive electrochemical membranes	100 mM KH_2PO_4; pH 4.5; flow rate 0.5 mL min^{-1}; 3.0V	10 μM atrazine	>99.9 (100min)	239
Bioelectrode-anaerobic sludge	-660 mV; 400mL; 35 °C	50 mg L^{-1} 2,4-	100(12h)	229

system		dichloronitrobenzene		
Nanofiltration- electrooxidation	14.9V; 20 °C; 50 A m^{-2}	870 mg L^{-1} PFHxA	~100 (1.47h)	240
O_3 -electrochemical coupled process	60 mA cm^{-2}; pH 3; 0.750L; ozone concentration 5 ± 0.5 mg L^{-1}	20 mg L^{-1} endosulfan	COD 95 (40min); TOC 94 (40min)	232
Electro-Fenton/BDD	80 mA cm^{-2}; flow rate 4 L min^{-1}; 3L; Fe^{2+} 0.5mM; 25 °C	300 mg L^{-1} reactive yellow HF	90(180min)	241
Photo-assisted electrochemical oxidation	2 g L^{-1} Na_2SO_4; pH 4.5 ± 0.2; flow rate of 1 L min^{-1}; 250 W HPL-N lamp	0.2 mg L^{-1} fluoroquinolone	76 (360min)	231
Hydrothermal electrocatalytic oxidation	50 mM Na_2SO_4; 0.2M H_2O_2; 0.55L; 5 mA cm^{-2}; 135 °C	100 mg L^{-1} 2,4-dichlorophenoxyacetic acid	93.7(90min); TOC 99.8(180min)	237
Bioelectrocatalysis system	Volume of single chamber 130mL; 55± 2 °C; mixed anaerobic seed sludge concentration ~3000 mg L^{-1}; hydraulic retention time 2 d;	0.4 mM p-fluoronitrobenzene	0.188 mM d^{-1}	242
Sonoelectrochemical system	0.1 M Na_2SO_4; frequency 380 kHz; 25±2 °C; 20 mA	0.025mM methylene blue	100 (1h)	234
nZVI and electrochemical reduction system	cathode 80 mL, anode 40mL; 2 g L^{-1} NaCl; 20 ±0.5 °C; 0.167 mA cm^{-2}	50 mg L^{-1} 2,4-dichlorophenoxyacetic Acid	87.6(4h)	243

The electro-Fenton (EF) process, namely the combination of electrochemical oxidation (EO) with the Fenton process, which usually electrogenerates Fenton's reagents (i.e., ferrous ion and hydrogen peroxide) in situ.[244,245] Compared with the traditional Fenton process, EF consumes fewer reagents and thus produces less iron sludge. Additionally, the EF process often exhibits higher activity than EO for the mineralization of HOPs. For example, Guzman and co-workers [241] employed both EO and EF to treat the reactive yellow HF dye, and they found that the •OH generated by the EF process removed more rapidly organic pollutants than EO. An interesting chapter by Oturan, N., and Oturan, M. A. keeps a close eye on important parameters of EF process, including principles, operational parameters, application, heterogeneous EF, and bioelectro-EF, which may benefit researchers in this field.[245]

Photocatalysis is another effective approach to eliminate pollutants from wastewater.[246] In the last few years, photocatalysis has shown to enhance the degradation efficiency of electrocatalysis.[231, 247-249] Generally, the following points can explain the synergistic effect. On the one hand, the external bias lead to a decline in the electron-hole recombination process and the UV-photons reaching the electrode surface form excited radicals. On the other hand, the photo irradiation can activate the electrochemically generated reactive radicals and overcome the mass-transport limitation.[249] To mineralize the norfloxacin in

wastewater, Salatiel and co-authors[231] found that the ultraviolet radiation could significantly improve the degradation performance of electrochemical oxidation. The coupling strategy possessed a higher TOC abatement (76%) than the direct photolysis (60%) and the electrochemical oxidation process (26%) in 360 min. In-depth analysis suggested that the increase in mineralization could be explained by a decrease in the electron-hole recombination on the TiO_2 phase of the electrode, and thus improving the generation of hydroxyl radicals.

In the traditional flow-by EO process, the diffusion of HOPs to the reaction zone is quite difficult, which results in a low mass transfer rate constant.[227] To overcome this mass transfer limitation, combining membrane filtration with the EO process in flow-through mode is an efficient method for HOPs mineralization. In this process, water moves through the pores on the designed electrode materials, which can minimize the thickness of the boundary layer, thus significantly upgrading the mass transfer rate of HOPs moving towards the electrode surface.[226, 227, 239] In a recent work, tubular porous Ti/SnO_2-Sb filters which possessed excellent electrochemical activity and penetration flux were worked as anodic reactive electrochemical membranes in a reactive electrochemical filter system.[227] The developed reactive electrochemical filter system in flow-through mode resulted in a higher RhB oxidation efficiency than the flow-by mode by 8.6-fold under the same operational conditions.

Bioelectrochemical systems (BESs) which based on the integration of the biological process and the electrochemical method have attracted increasing attention in the HOPs degradation process because the BES process possesses high degradation efficiency, low operational cost, environmental sustainability, high selectivity, ambient operating conditions and reusable effluents.[242, 250] In a typical study, a coupled microbial electrosynthesis-upflow anaerobic sludge reactor (MES-UASB) was established to mineralize 2,4-dichloronitrobenzene,[229] and the experimental results indicated that the coupled MES-UASB obtained a high

dechlorination efficiency (100%) at -660 mV in 12h. More information involves this topic can be found in pervious reviews and chapters.[250-253]

5. Conclusions and prospects

In this work, the recent development of electrocatalysts for the degradation of HOPs in terms of the strategies for promoting the catalysts activities is comprehensively reviewed. It can be concluded that both electrooxidation and electroreduction are effective strategies to mineralize HOPs, with the application of adequate catalysts.

In the electrooxidative process, metal oxides (e.g., PbO_2 and SnO_2) and BDD are extensively applied as anodes due to their high performance in the production of •OH that is the main reactive radical in the oxidation degradation pathway. Additionally, nanostructuring, compositing, doping, and surface modification are extensively used stategies to upgrade the ability of these catalysts. Notably, the oxidation mechanisms that involve •OH rely heavily on the properties of catalysts. For the active anodes (e.g., Pt, RuO_2, IrO_2), the degradation process often leads to electrochemical conversion, while the inactive anodes (e.g., BDD, doped-SnO_2, PbO_2) commonly result in electrochemical combustion.

In the electroreductive process, metals (e.g., Ag and Pd) and low-valent metal complexes are responsible for the reduction of HOPs through the generated •H and electrons. To obtain a better degradation performance, many sound methods such as nanosizing, structure designing, alloying, and component modification are extensively introduced. The reduction principles are closely related to the type of catalysts. The dissociative electron transfer (DET) theory can account for vast experimental phenomena when Ag-based cathodes are used. The homogeneous ET process will occur when electrogenerated low-valent metal complexes are employed as catalysts. In addition, the application of Pd-based catalysts is an indirect dehalogenation process, with the H^*_{ads} acting as the main active radical.

View Article Online
DOI: 10.1039/C9EN00411D

Identifying the structure-performance relationship of materials is crucial to the design of desirable electrocatalysts. For the electrochemical dehalogenation process, both activity and stability of catalysts need to be considered carefully. As aforementioned, nanostructuring, compositing, component regulation (doping, alloying), inserting interlayer, and surface modification have shown great potential in designing robust and highly active electrocatalysts. Nanostructuring catalysts with well- dispersed active components that exhibit a high active surface area can provide more sites for the degradation reaction. Compositing also leads to a high specific surface area, specially, when a conductive substrate is involved, the conductivity and mass transfer process can be significantly elevated, and thus accelerating the degradation process. Component regulation, such as doping and alloying, usually results in more abundant active components on catalyst surfaces, and thereby benefits the generation of more active radicals for the decomposition reaction. In addition, the optimal components possess a decent interaction strength with radicals (e.g., H*, •OH), and diminish the side reactions (e.g., oxygen and hydrogen evolution reactions). Interlayer and surface modification have a significant impact on the lifetime of electrocatalysts by hindering the penetration of electrolytes, decreasing the inner mechanical stress, and preventing the catalyst damages (e.g., detachment, consumption, dissolution). Other strategies that mentioned above also benefit the durability of catalysts.

However, more innovative catalysts and technological methods are still highly desired for the further development of electrocatalytic dehalogenation process due to some critical limitations/challenges related to the practical application of the current electrocatalytic dehalogenation treatment.[1, 28, 254] Firstly, the electricity is required continuously to support the electrochemical degradation process, and the electrical efficiency should be checked when evaluating the applicability of the electrocatalysis techniques. To decrease the energy cost, integrating electrocatalysis with other renewable energy techniques (e.g., solar photovoltaic

power) and optimizing the operational parameters are highly advisable. Another interesting factor is the wastewater conductivity, which can be enhanced through the addition of seawater and inorganic salts (e.g., Na_2SO_4, phosphate buffer, Na_2CO_3). Secondly, the released toxic ions (e.g., Pb^{2+}) of electrodes may decrease the durability of electrodes and pose toxicity toward organisms, while the fouling and corrosion of electrodes (e.g., BDD) may also lead to an unstable degradation efficiency. These factors could hinder the industrial applications of the electrocatalytic degradation method. As a result, the robust and highly active electrodes are extremely needed. Thirdly, the formation of toxic by-products in the degradation of HOPs, especially halogen-based compounds (e.g., BrO_3^-, ClO_3^-, ClO_4^-), can limit the adoption of the electrochemical mineralization techniques. To control the generation of these products, the optimal operational strategies and the efficient electrode modifications are necessary. Currently, the electrocatalysis has been extensively studied in the mineralization of pollutants beyond HOPs, while the degradation of real wastewater is still limited. Consequently, it is of great significance to explore the potential application of electrochemical method in degrading complex pollutants in industrial wastewater. As indicated, the controllable electroreduction of organic pollutants can lead to the transformation of pollutants into value-added chemicals, for example the generation of n-hexane from the degradation of 1, 2-dibromohexane. Accordingly, the electrochemical method is a promising approach to generate valuable chemicals with specific functional groups. In summary, a combination of hybrid technologies, ideal operating conditions, and electrode modifications needs to be explored to address these crucial challenges.

Herein, several prospects are listed below for the purpose of upgrading existing electrochemical degradation techniques.

Developing high-performance catalysts is of great importance and many strategies including doping, nanostructuring, facet engineering, hybrid engineering, defect engineering, and

View Article Online
DOI: 10.1039/C9EN00411D

alloying are efficient ways to improve the activity of catalysts. Furthermore, the structure-performance relationship should be taken seriously with the help of computational methods, and high-through screening is also vital to select typical catalysts for a determined pollutant. Another factor should be taken into consideration is the cost. More efforts should be devoted to using those low-cost materials (e.g., non-precious metals, graphite-based materials) and simple fabrication methods to obtain cost-effective electrodes.

To maximize the performance of electrocatalysts, it is necessary to optimize the experimental parameters in the degradation process. Normally, a reactor/system with a high electrode area to volume ratio, a low cell voltage, and a high mass transport rate is desired.[2] As discussed aforementioned, the role of current, voltage, pH, electrolyte, and concentration of HOPs is also vital to the activity of catalysts, as well as the degradation pathway. Hence, systematic investigations should be conducted to achieve better mineralization efficiency.

Advancing the scientific understanding of dehalogenation/electrochemical process is still a key challenge, and the mechanism should be investigated case by case with the experimental and theoretical methods, especially those operando characterization techniques. The applications of advanced in situ characterization techniques have benefited a lot for exploring the active sites on electrocatalysts for various reactions.[255] For instance, the advanced scanning electrochemical microscopy technique can offer spatially resolved details of electrode reactivity at the micron to submicron scale, which is highly beneficial for characterizing the performance of catalysts and identifying mechanisms involves HOPs transformation.[108] This process could also leads to the design of more favorable catalysts. Additionally, the theoretical study based on density functional theory can provide critical information to understand the interaction between catalysts/radicals and pollutants, thus leading to a better understanding of the degradation/mineralization process.[220, 256, 257]

Taking advantages of other useful processes for HOPs degradation, coupling electrocatalysis with those sophisticated methods will significantly upgrade the degradation performance. On one side, to achieve better degradation efficiencies, integrating those verified effective techniques such as membrane techniques, biological methods, Fenton processes, and photocatalysis with electrocatalysis is a promising solution. On the other hand, to decrease the operational cost, mainly the electricity utilization, it is advisable to investigate the combination the electrochemical degradation process with renewable energy (e.g., solar photovoltaic power, wave power, wind energy, geothermal energy) in future research.

Acknowledgments

This work is supported by an Australian Research Council (ARC) Future Fellowship (FT160100195). Mr Zhijie Chen acknowledges the China Scholarship Council (CSC) for the scholarship support.

References

1. S. Rondinini, C. Locatelli, A. Minguzzi and A. Vertova, Electroreduction, in *Electrochemical Water and Wastewater Treatment*, 2018, DOI: 10.1016/b978-0-12-813160-2.00001-8, pp. 3-28.
2. E. T. Martin, C. M. McGuire, M. S. Mubarak and D. G. Peters, Electroreductive Remediation of Halogenated Environmental Pollutants, *Chem. Rev.*, 2016, **116**, 15198-15234.
3. P. Kar and B. G. Mishra, Potential application of Pd-Ni bimetallic nanoparticles dispersed in Al-pillared clay matrix as catalyst for hydrodechlorination of chloroanilines from aqueous sources, *J. Environ. Chem. Eng.*, 2016, **4**, 1962-1969.
4. C. K. O. da Silva-Rackov, W. A. Lawal, P. A. Nfodzo, M. M. G. R. Vianna, C. A. O. do Nascimento and H. Choi, Degradation of PFOA by hydrogen peroxide and persulfate activated by iron-modified diatomite, *Appl. Catal. B-Environ.*, 2016, **192**, 253-259.

5. A. Yazdanbakhsh, A. Eslami, G. Moussavi, M. Rafiee and A. Sheikhmohammadi, Photo-assisted degradation of 2, 4, 6-trichlorophenol by an advanced reduction process based on sulfite anion radical: Degradation, dechlorination and mineralization, *Chemosphere*, 2018, **191**, 156-165.

6. C. Zhang, D. Zhang, Z. Li, T. Akatsuka, S. Yang, D. Suzuki and A. Katayama, Insoluble Fe-Humic Acid Complex as a Solid-Phase Electron Mediator for Microbial Reductive Dechlorination, *Environ. Sci. Technol.*, 2014, **48**, 6318-6325.

7. L. Yu, Y. Yuan, J. Tang, Y. Wang and S. Zhou, Biochar as an electron shuttle for reductive dechlorination of pentachlorophenol by Geobacter sulfurreducens, *Sci. Rep.*, 2015, **5**, 16221.

8. L. Wang, B. Batchelor, S. D. Pillai and V. S. V. Botlaguduru, Electron beam treatment for potable water reuse: Removal of bromate and perfluorooctanoic acid, *Chem. Eng. J.*, 2016, **302**, 58-68.

9. M. Trojanowicz, I. Bartosiewicz, A. Bojanowska-Czajka, K. Kulisa, T. Szreder, K. Bobrowski, H. Nichipor, J. F. Garcia-Reyes, G. Nałęcz-Jawecki, S. Męczyńska-Wielgosz and J. Kisała, Application of ionizing radiation in decomposition of perfluorooctanoate (PFOA) in waters, *Chem. Eng. J.*, 2019, **357**, 698-714.

10. R. Wang, T. Tang, G. Lu, K. Huang, H. Yin, Z. Lin, F. Wu and Z. Dang, Rapid debromination of polybrominated diphenyl ethers (PBDEs) by zero valent metal and bimetals: Mechanisms and pathways assisted by density function theory calculation, *Environ. Pollut.*, 2018, **240**, 745-753.

11. B. Vanrenterghem, P. Jovanovič, M. Šala, M. Bele, V. S. Šelih, N. Hodnik and T. Breugelmans, Stability study of silver nanoparticles towards the halide electroreduction, *Electrochim. Acta*, 2018, **286**, 123-130.

12. S. Chen, W. Chu, H. Wei, H. Zhao, B. Xu, N. Gao and D. Yin, Reductive dechlorination of haloacetamides in drinking water by Cu/Fe bimetal, *Sep. Purif. Technol.*, 2018, **203**, 226-232.

13. R. P. Milstead, K. T. Nance, K. S. Tarnas, K. E. Egelhofer and D. R. Griffith, Photochemical degradation of halogenated estrogens under natural solar irradiance, *Environ. Sci. Proc. Imp.*, 2018, **20**, 1350-1360.

14. R. Wang, T. Tang, J. Xie, X. Tao, K. Huang, M. Zou, H. Yin, Z. Dang and G. Lu, Debromination of polybrominated diphenyl ethers (PBDEs) and their conversion to polybrominated dibenzofurans (PBDFs) by UV light: Mechanisms and pathways, *J. Hazard. Mater.*, 2018, **354**, 1-7.

15. R. Qu, C. Li, J. Liu, R. Xiao, X. Pan, X. Zeng, Z. Wang and J. Wu, Hydroxyl Radical Based Photocatalytic Degradation of Halogenated Organic Contaminants and Paraffin on Silica Gel, *Environ. Sci. Technol.*, 2018, **52**, 7220-7229.

16. J. C. Lin, C. Y. Hu and S. L. Lo, Effect of surfactants on the degradation of perfluorooctanoic acid (PFOA) by ultrasonic (US) treatment, *Ultrason. Sonochem.*, 2016, **28**, 130-135.

17. J. Cheng, C. D. Vecitis, H. Park, B. T. Mader and M. R. Hoffmann, Sonochemical degradation of perfluorooctane sulfonate (PFOS) and perfluorooctanoate (PFOA) in groundwater: kinetic effects of matrix inorganics, *Environ. Sci. Technol.*, 2010, **44**, 445-450.

18. Z. Lou, Y. Li, J. Zhou, K. Yang, Y. Liu, S. A. Baig and X. Xu, TiC doped palladium/nickel foam cathode for electrocatalytic hydrodechlorination of 2,4-DCBA: Enhanced electrical conductivity and reactive activity, *J. Hazard. Mater.*, 2019, **362**, 148-159.

19. M. Yan, Z. Chen, N. Li, Y. Zhou, C. Zhang and G. Korshin, Electrochemical reductive dehalogenation of iodine-containing contrast agent pharmaceuticals: Examination of reactions of diatrizoate and iopamidol using the method of rotating ring-disc electrode (RRDE), *Water Res.*, 2018, **136**, 104-111.

20. K. Zhu, X. Wang, X. Ma, Z. Sun and X. Hu, Comparative Degradation of Atrazine by Anodic Oxidation at Graphite and Platinum Electrodes and Insights into Electrochemical Behavior of Graphite Anode, *Electrocatalysis*, 2019, **10**, 35-44.

21. E. M. Siedlecka, A. Ofiarska, A. F. Borzyszkowska, A. Bialk-Bielinska, P. Stepnowski and A. Pieczynska, Cytostatic drug removal using electrochemical oxidation with BDD electrode: Degradation pathway and toxicity, *Water Res.*, 2018, **144**, 235-245.

22. M. Trojanowicz, A. Bojanowska-Czajka, I. Bartosiewicz and K. Kulisa, Advanced Oxidation/Reduction Processes treatment for aqueous perfluorooctanoate (PFOA) and

perfluorooctanesulfonate (PFOS) - A review of recent advances, *Chem. Eng. J.*, 2018, **336**, 170-199.

23. Q. Li, Q. Zhang, H. Cui, L. Ding, Z. Wei and J. Zhai, Fabrication of cerium-doped lead dioxide anode with improved electrocatalytic activity and its application for removal of Rhodamine B, *Chem. Eng. J.*, 2013, **228**, 806-814.
24. C. Fang, M. Megharaj and R. Naidu, Electrochemical Advanced Oxidation Processes (EAOP) to degrade per- and polyfluoroalkyl substances (PFASs), *J. Adv. Oxid. Technol.*, 2017, **20**.
25. C. A. Martínez-Huitle and E. Brillas, Decontamination of wastewaters containing synthetic organic dyes by electrochemical methods: A general review, *Appl. Catal. B-Environ.*, 2009, **87**, 105-145.
26. E. Brillas and C. A. Martínez-Huitle, Decontamination of wastewaters containing synthetic organic dyes by electrochemical methods. An updated review, *Appl. Catal. B-Environ.*, 2015, **166-167**, 603-643.
27. I. Ross, J. McDonough, J. Miles, P. Storch, P. Thelakkat Kochunarayanan, E. Kalve, J. Hurst, S. S. Dasgupta and J. Burdick, A review of emerging technologies for remediation of PFASs, *Remediation J.*, 2018, **28**, 101-126.
28. J. Niu, Y. Li, E. Shang, Z. Xu and J. Liu, Electrochemical oxidation of perfluorinated compounds in water, *Chemosphere*, 2016, **146**, 526-538.
29. G. Korshin and M. Yan, Electrochemical dehalogenation of disinfection by-products and iodine-containing contrast media: A review, *Environ. Eng. Res.*, 2018, **23**, 345-353.
30. F. Geneste, Catalytic electrochemical pre-treatment for the degradation of persistent organic pollutants, *Curr. Opin. Electrochem.*, 2018, DOI: 10.1016/j.coelec.2018.07.002.
31. E. Duñach, M. J. Medeiros and S. Olivero, Electrochemical cyclizations of organic halides catalyzed by electrogenerated nickel(I) complexes: towards environmentally friendly methodologies, *Electrochim. Acta*, 2017, **242**, 373-381.
32. C. M. M. Dennis G. Peters, Erick M. Pasciak, Angela A. Peverly, Lauren M. Strawsine, Elizabeth R. Wagoner, and J. Tyler Barnes, Electrochemical Dehalogenation of Organic Pollutants, *J. Mex. Chem. Soc.*, 2014, **58**, 287-302.

33. H. Yu, Y. Song, B. Zhao, Y. Lu, S. Zhu, J. Qu, X. Wang and W. Qin, Efficient Electrocatalytic Degradation of 4-Chlorophenol Using a Ti/RuO_2-SnO_2-TiO_2/PbO_2-CeO_2 Composite Electrode, *Electrocatalysis*, 2018, **9**, 725-734.

34. Y. Yao, C. Huang, Y. Yang, M. Li and B. Ren, Electrochemical removal of thiamethoxam using three-dimensional porous PbO_2-CeO_2 composite electrode: Electrode characterization, operational parameters optimization and degradation pathways, *Chem. Eng. J.*, 2018, **350**, 960-970.

35. Q. Zhang, X. Guo, X. Cao, D. Wang and J. Wei, Facile preparation of a Ti/α-PbO_2/β-PbO_2 electrode for the electrochemical degradation of 2-chlorophenol, *Chinese J. Catal.*, 2015, **36**, 975-981.

36. X. Duan, C. Zhao, W. Liu, X. Zhao and L. Chang, Fabrication of a novel PbO_2 electrode with a graphene nanosheet interlayer for electrochemical oxidation of 2-chlorophenol, *Electrochim. Acta*, 2017, **240**, 424-436.

37. Q. Zhuo, Q. Xiang, H. Yi, Z. Zhang, B. Yang, K. Cui, X. Bing, Z. Xu, X. Liang, Q. Guo and R. Yang, Electrochemical oxidation of PFOA in aqueous solution using highly hydrophobic modified PbO_2 electrodes, *J. Electroanal. Chem.*, 2017, **801**, 235-243.

38. H. Lin, J. Niu, S. Ding and L. Zhang, Electrochemical degradation of perfluorooctanoic acid (PFOA) by Ti/SnO_2-Sb, Ti/SnO_2-Sb/PbO_2 and Ti/SnO_2-Sb/MnO_2 anodes, *Water Res.*, 2012, **46**, 2281-2289.

39. C. Wang, J. Niu, L. Yin, J. Huang and L.-A. Hou, Electrochemical degradation of fluoxetine on nanotube array intercalated anode with enhanced electronic transport and hydroxyl radical production, *Chem. Eng. J.*, 2018, **346**, 662-671.

40. Z. Xu, Y. Yu, H. Liu and J. Niu, Highly efficient and stable Zr-doped nanocrystalline PbO_2 electrode for mineralization of perfluorooctanoic acid in a sequential treatment system, *Sci. Total Environ.*, 2017, **579**, 1600-1607.

41. Z. He, J. Zhou, X. Huang, S. Zhang and S. Song, Enhancement of the Activity and Stability of PbO_2 Electrodes by Modifying with Polydimethylsiloxane, *J. Electrochem. Soc.*, 2018, **165**, H717-H724.

42. X. Zhu, M. Tong, S. Shi, H. Zhao and J. Ni, Essential explanation of the strong mineralization performance of boron-doped diamond electrodes, *Environ. Sci. Technol.*, 2008, **42**, 4914-4920.

43. C. Wang, L. Yin, Z. Xu, J. Niu and L.-A. Hou, Electrochemical degradation of enrofloxacin by lead dioxide anode: Kinetics, mechanism and toxicity evaluation, *Chem. Eng. J.*, 2017, **326**, 911-920.

44. Y. Yao, G. Teng, Y. Yang, C. Huang, B. Liu and L. Guo, Electrochemical oxidation of acetamiprid using Yb-doped PbO_2 electrodes: Electrode characterization, influencing factors and degradation pathways, *Sep. Purif. Technol.*, 2019, **211**, 456-466.

45. Y. Yao, L. Jiao, L. Cui, N. Yu, F. Wei and Z. Lu, Preparation and Characterization of PbO_2-CeO_2 Nanocomposite Electrode with High Cerium Content and Its Appplication in the Electrocatalytic Degradation of Malachite Green, *J. Electrochem. Soc.*, 2015, **162**, H693-H698.

46. J. Kong, S. Shi, L. Kong, X. Zhu and J. Ni, Preparation and characterization of PbO2 electrodes doped with different rare earth oxides, *Electrochim. Acta*, 2007, **53**, 2048-2054.

47. C. Yang, Y. Wang, B. Hu, H. Zhang, Y. Lv and X. Zhou, Optimized Fabrication of TiO_2 Nanotubes Array/SnO_2-Sb/Fe-Doped PbO_2 Electrode and Application in Electrochemical Treatment of Dye Wastewater, *J. Electron. Mater.*, 2018, **47**, 5965-5972.

48. J. Chen, Y. Xia and Q. Dai, Electrochemical degradation of chloramphenicol with a novel Al doped PbO_2 electrode: Performance, kinetics and degradation mechanism, *Electrochim. Acta*, 2015, **165**, 277-287.

49. Y. Song, G. Wei and R. Xiong, Structure and properties of PbO_2-CeO_2 anodes on stainless steel, *Electrochim. Acta*, 2007, **52**, 7022-7027.

50. Y. Yao, C. Zhao and J. Zhu, Preparation and characterization of PbO2–ZrO2 nanocomposite electrodes, *Electrochim. Acta*, 2012, **69**, 146-151.

51. Y. Yao, C. Zhao, M. Zhao and X. Wang, Electrocatalytic degradation of methylene blue on PbO_2-ZrO_2 nanocomposite electrodes prepared by pulse electrodeposition, *J. Hazard. Mater.*, 2013, **263 Pt 2**, 726-734.

52. H. Du, G. Duan, N. Wang, J. Liu, Y. Tang, R. Pang, Y. Chen and P. Wan, Fabrication of Ga_2O_3-PbO_2 electrode and its performance in electrochemical advanced oxidation processes, *J. Solid State Electr.*, 2018, **22**, 3799-3806.

53. Y. Yao, M. Zhao, C. Zhao and H. Zhang, Preparation and properties of PbO_2-ZrO_2 nanocomposite electrodes by pulse electrodeposition, *Electrochim. Acta*, 2014, **117**, 453-459.

54. G. Zhao, Y. Zhang, Y. Lei, B. Lv, J. Gao, Y. Zhang and D. Li, Fabrication and electrochemical treatment application of a novel lead dioxide anode with superhydrophobic surfaces, high oxygen evolution potential, and oxidation capability, *Environ. Sci. Technol.*, 2010, **44**, 1754-1759.

55. X. Duan, F. Ma, Z. Yuan, L. Chang and X. Jin, Lauryl benzene sulfonic acid sodium-carbon nanotube-modified PbO_2 electrode for the degradation of 4-chlorophenol, *Electrochim. Acta*, 2012, **76**, 333-343.

56. Q. Zhuo, M. Luo, Q. Guo, G. Yu, S. Deng, Z. Xu, B. Yang and X. Liang, Electrochemical Oxidation of Environmentally Persistent Perfluorooctane Sulfonate by a Novel Lead Dioxide Anode, *Electrochim. Acta*, 2016, **213**, 358-367.

57. N. Wachter, J. M. Aquino, M. Denadai, J. C. Barreiro, A. J. Silva, Q. B. Cass, R. C. Rocha-Filho and N. Bocchi, Optimization of the electrochemical degradation process of the antibiotic ciprofloxacin using a double-sided β-PbO_2 anode in a flow reactor: kinetics, identification of oxidation intermediates and toxicity evaluation, *Environ. Sci. Pollut. Res. Int.*, 2018, **26**, 4438-4449.

58. S. Liu, X. Zhou, W. Han, J. Li, X. Sun, J. Shen and L. Wang, Theoretical and experimental insights into the ·OH-mediated mineralization mechanism of flutriafol, *Electrochim. Acta*, 2017, **235**, 223-232.

59. S. Liu, Y. Wang, X. Zhou, W. Han, J. Li, X. Sun, J. Shen and L. Wang, Improved degradation of the aqueous flutriafol using a nanostructure macroporous PbO_2 as reactive electrochemical membrane, *Electrochim. Acta*, 2017, **253**, 357-367.

60. Y. Xia and Q. Dai, Electrochemical degradation of antibiotic levofloxacin by PbO_2 electrode: Kinetics, energy demands and reaction pathways, *Chemosphere*, 2018, **205**, 215-222.

61. F. d. A. A. d. Figueredo-Sobrinho, F. W. d. S. Lucas, T. P. Fill, E. Rodrigues-Filho, I. H. Mascaro, P. N. d. S. Casciano, P. d. Lima-Neto and A. N. Correia, Insights into electrodegradation mechanism of tebuconazole pesticide on Bi-doped PbO_2 electrodes, *Electrochim. Acta*, 2015, **154**, 278-286.

62. I. Sánchez-Montes, J. R. Fuzer Neto, B. F. Silva, A. J. Silva, J. M. Aquino and R. C. Rocha-Filho, Evolution of the antibacterial activity and oxidation intermediates during the electrochemical degradation of norfloxacin in a flow cell with a PTFE-doped β-PbO_2 anode: Critical comparison to a BDD anode, *Electrochim. Acta*, 2018, **284**, 260-270.

63. R. Xie, X. Meng, P. Sun, J. Niu, W. Jiang, L. Bottomley, D. Li, Y. Chen and J. Crittenden, Electrochemical oxidation of ofloxacin using a TiO_2-based SnO_2-Sb/polytetrafluoroethylene resin-PbO_2 electrode: Reaction kinetics and mass transfer impact, *Appl. Catal. B-Environ.*, 2017, **203**, 515-525.

64. H. Liu, S. Yu, T. Shen, S. Tong and C. Ma, Preparation of a high-performance composite PbO_2 electrode from a new bath for p-chlorophenol oxidation, *Sep. Purif. Technol.*, 2014, **132**, 27-32.

65. S. Y. Yang, Y. S. Choo, S. Kim, S. K. Lim, J. Lee and H. Park, Boosting the electrocatalytic activities of SnO_2 electrodes for remediation of aqueous pollutants by doping with various metals, *Appl. Catal. B-Environ.*, 2012, **111-112**, 317-325.

66. M. Panizza and G. Cerisola, Direct and mediated anodic oxidation of organic pollutants, *Chem. Rev.*, 2009, **109**, 6541-6569.

67. Q. Zhuo, S. Deng, B. Yang, J. Huang and G. Yu, Efficient electrochemical oxidation of perfluorooctanoate using a Ti/SnO_2-Sb-Bi anode, *Environ. Sci. Technol.*, 2011, **45**, 2973-2979.

68. Y. Wang, C. Shen, M. Zhang, B.-T. Zhang and Y.-G. Yu, The electrochemical degradation of ciprofloxacin using a SnO_2 -Sb/Ti anode: Influencing factors, reaction pathways and energy demand, *Chem. Eng. J.*, 2016, **296**, 79-89.

69. B. Yang, J. Wang, C. Jiang, J. Li, G. Yu, S. Deng, S. Lu, P. Zhang, C. Zhu and Q. Zhuo, Electrochemical mineralization of perfluorooctane sulfonate by novel F and Sb co-doped Ti/SnO_2 electrode containing Sn-Sb interlayer, *Chem. Eng. J.*, 2017, **316**, 296-304.

70. T. Duan, Y. Chen, Q. Wen and Y. Duan, Enhanced electrocatalytic activity of nano-TiN composited Ti/Sb-SnO_2 electrode fabricated by pulse electrodeposition for methylene blue decolorization, *RSC Adv.*, 2014, **4**, 57463-57475.

71. H. Lin, J. Niu, J. Xu, H. Huang, D. Li, Z. Yue and C. Feng, Highly efficient and mild electrochemical mineralization of long-chain perfluorocarboxylic acids (C9-C10) by Ti/SnO_2-Sb-Ce, Ti/SnO_2-Sb/Ce-PbO_2, and Ti/BDD electrodes, *Environ. Sci. Technol.*, 2013, **47**, 13039-13046.

72. W. F. Chen, J. T. Muckerman and E. Fujita, Recent developments in transition metal carbides and nitrides as hydrogen evolution electrocatalysts, *Chem. Commun. (Camb)*, 2013, **49**, 8896-8909.

73. J. G. Chen, Carbide and Nitride Overlayers on Early Transition Metal Surfaces: Preparation, Characterization, and Reactivities, *Chem. Rev.*, 1996, **96**, 1477-1498.

74. M. Shestakova, P. Bonete, R. Gómez, M. Sillanpää and W. Z. Tang, Novel Ti/Ta_2O_5-SnO_2 electrodes for water electrolysis and electrocatalytic oxidation of organics, *Electrochim. Acta*, 2014, **120**, 302-307.

75. H. Bai, P. He, J. Chen, K. Liu, H. Lei, X. Zhang, F. Dong and H. Li, Electrocatalytic degradation of bromocresol green wastewater on Ti/SnO_2-RuO_2 electrode, *Water Sci. Technol.*, 2017, **75**, 220-227.

76. R. Vargas, S. Díaz, L. Viele, O. Núñez, C. Borrás, J. Mostany and B. R. Scharifker, Electrochemical oxidation of dichlorvos on SnO_2-Sb_2O_5 electrodes, *Appl. Catal. B-Environ.*, 2014, **144**, 107-111.

77. B. Tang, H. Shi, Z. Fan and G. Zhao, Preferential electrocatalytic degradation of 2,4-dichlorophenoxyacetic acid on molecular imprinted mesoporous SnO_2 surface, *Chem. Eng. J.*, 2018, **334**, 882-890.

78. M. Abbasi, J. Bäckström and A. Cornell, Fabrication of Spin-Coated Ti/TiH_x/Ni-Sb-SnO_2 Electrode: Stability and Electrocatalytic Activity, *J. Electrochem. Soc.*, 2018, **165**, H568-H574.

79. M. Shestakova, J. Graves, M. Sitarz and M. Sillanpää, Optimization of Ti/Ta_2O_5-SnO_2 electrodes and reaction parameters for electrocatalytic oxidation of methylene blue, *J. Appl. Electrochem.*, 2016, **46**, 349-358.

80. B. Yang, C. Jiang, G. Yu, Q. Zhuo, S. Deng, J. Wu and H. Zhang, Highly efficient electrochemical degradation of perfluorooctanoic acid (PFOA) by F-doped Ti/SnO_2 electrode, *J. Hazard. Mater.*, 2015, **299**, 417-424.

81. Q. Zhuo, X. Li, F. Yan, B. Yang, S. Deng, J. Huang and G. Yu, Electrochemical oxidation of 1H,1H,2H,2H-perfluorooctane sulfonic acid (6:2 FTS) on DSA electrode: operating parameters and mechanism, *J. Environ. Sci. (China)*, 2014, **26**, 1733-1739.

82. T. Duan, Q. Wen, Y. Chen, Y. Zhou and Y. Duan, Enhancing electrocatalytic performance of Sb-doped SnO_2 electrode by compositing nitrogen-doped graphene nanosheets, *J. Hazard. Mater.*, 2014, **280**, 304-314.

83. H. Zhao, J. Gao, G. Zhao, J. Fan, Y. Wang and Y. Wang, Fabrication of novel SnO_2-Sb/carbon aerogel electrode for ultrasonic electrochemical oxidation of perfluorooctanoate with high catalytic efficiency, *Appl. Catal. B-Environ.*, 2013, **136-137**, 278-286.

84. S. Chai, Y. Wang, Y.-n. Zhang, H. Zhao, M. Liu and G. Zhao, Construction of a bifunctional electrode interface for efficient electrochemical mineralization of recalcitrant pollutants, *Appl. Catal. B-Environ.*, 2018, **237**, 473-481.

85. M. M. Petrović, J. Z. Mitrović, M. D. Radović, M. M. Kostić and A. L. J. Bojić, Preparation and characterisation of a new stainless steel/Bi_2O_3 anode and its dyes degradation ability, *Can. J. Chem. Eng.*, 2014, **92**, 1000-1007.

86. R. Kaur, J. P. Kushwaha and N. Singh, Electro-oxidation of Ofloxacin antibiotic by dimensionally stable Ti/RuO_2 anode: Evaluation and mechanistic approach, *Chemosphere*, 2018, **193**, 685-694.

87. S. Agnihotri, P. Kaur, V. K. Sangal, A. Garg and A. Verma, Parametric Study for the Treatment of Simulated Cetirizine Wastewater Using Electrochemical Methods: Optimization and Cost Analysis, *J. Electrochem. Soc.*, 2018, **165**, E556-E562.

88. Y.-M. Z. Rita FaridaYunus, K. G. Nadeeshani Nanayakkara, and J. Paul Chen, Electrochemical Removal of Rhodamine 6G by Using RuO_2 Coated Ti DSA, *Ind. Eng. Chem. Res.*, 2009, **48**, 7466-7473.

89. Y. Zhang, T. Yu, W. Han, X. Sun, J. Li, J. Shen and L. Wang, Electrochemical treatment of anticancer drugs wastewater containing 5-Fluoro-2-Methoxypyrimidine using a tubular porous electrode electrocatalytic reactor, *Electrochim. Acta*, 2016, **220**, 211-221.

90. S. You, B. Liu, Y. Gao, Y. Wang, C. Y. Tang, Y. Huang and N. Ren, Monolithic Porous Magnéli-phase Ti_4O_7 for Electro-oxidation Treatment of Industrial Wastewater, *Electrochim. Acta*, 2016, **214**, 326-335.

91. J. Wang, D. Zhi, H. Zhou, X. He and D. Zhang, Evaluating tetracycline degradation pathway and intermediate toxicity during the electrochemical oxidation over a Ti/Ti_4O_7 anode, *Water Res.*, 2018, **137**, 324-334.

92. H. Lin, J. Niu, S. Liang, C. Wang, Y. Wang, F. Jin, Q. Luo and Q. Huang, Development of macroporous Magnéli phase Ti_4O_7 ceramic materials: As an efficient anode for mineralization of poly- and perfluoroalkyl substances, *Chem. Eng. J.*, 2018, **354**, 1058-1067.

93. C. Lyu, J. Zheng, R. Zhang, R. Zou, B. Liu and W. Zhou, Homologous Co_3O_4‖CoP nanowires grown on carbon cloth as a high-performance electrode pair for triclosan degradation and hydrogen evolution, *Mater. Chem. Front.*, 2018, **2**, 323-330.

94. S. D. Jojoa-Sierra, J. Silva-Agredo, E. Herrera-Calderon and R. A. Torres-Palma, Elimination of the antibiotic norfloxacin in municipal wastewater, urine and seawater by electrochemical oxidation on IrO_2 anodes, *Sci. Total Environ.*, 2017, **575**, 1228-1238.

95. M. M. Petrović, I. J. Slipper, M. D. Antonijević, G. S. Nikolić, J. Z. Mitrović, D. V. Bojić and A. L. Bojić, Characterization of a Bi_2O_3 coat based anode prepared by galvanostatic electrodeposition and its use for the electrochemical degradation of Reactive Orange 4, *J. Taiwan Inst. Chem. E.*, 2015, **50**, 282-287.

96. J. De Coster, W. Vanherck, L. Appels and R. Dewil, Selective electrochemical degradation of 4-chlorophenol at a Ti/RuO_2-IrO_2 anode in chloride rich wastewater, *J. Environ. Manage.*, 2017, **190**, 61-71.

97. L. Du, J. Wu and C. Hu, Electrochemical oxidation of Rhodamine B on RuO_2-PdO-TiO_2/Ti electrode, *Electrochim. Acta*, 2012, **68**, 69-73.

98. A. Rossi, V. A. Alves, L. A. Da Silva, M. A. Oliveira, D. O. S. Assis, F. A. Santos and R. R. S. De Miranda, Electrooxidation and inhibition of the antibacterial activity of oxytetracycline hydrochloride using a RuO_2 electrode, *J. Appl. Electrochem.*, 2008, **39**, 329-337.

99. M. Petrovic, J. Mitrovic, M. Radovic, D. Bojic, M. Kostic, R. Ljupkovic and A. Bojic, Synthesis of bismuth (III) oxide films based anodes for electrochemical degradation of reactive blue 19 and crystal violet, *Hem. Ind.*, 2014, **68**, 585-595.

100. A. Urtiaga, A. Soriano and J. Carrillo-Abad, BDD anodic treatment of 6:2 fluorotelomer sulfonate (6:2 FTSA). Evaluation of operating variables and by-product formation, *Chemosphere*, 2018, **201**, 571-577.

101. E. Peralta, Degradation of 4-Chlorophenol in a Batch Electrochemical Reactor Using BDD Electrodes, *Int. J. Electrochem. Sci.*, 2018, **13**, 4625-4639.

102. P. Kariyajjanavar, J. Narayana and Y. A. Nayaka, Degradation of textile dye C.I. Vat Black 27 by electrochemical method by using carbon electrodes, *J. Environ. Chem. Eng.*, 2013, **1**, 975-980.

103. N. Li, S. Dong, W. Lv, S. Huang, H. Chen, Y. Yao and W. Chen, Enhanced electrocatalytic oxidation of dyes in aqueous solution using cobalt phthalocyanine modified activated carbon fiber anode, *Sci. China Chem.*, 2013, **56**, 1757-1764.

104. H. Liu, Z. Zhang, M. Ren, J. Guan, N. Lu, J. Qu, X. Yuan and Y. N. Zhang, Preparation of the CNTs/AG/ITO electrode with high electro-catalytic activity for 2-chlorophenol degradation and the potential risks from intermediates, *J. Hazard. Mater.*, 2018, **359**, 148-156.

105. E. Pajootan and M. Arami, Structural and electrochemical characterization of carbon electrode modified by multi-walled carbon nanotubes and surfactant, *Electrochim. Acta*, 2013, **112**, 505-514.

106. Z. Liu, F. Wang, Y. Li, T. Xu and S. Zhu, Continuous electrochemical oxidation of methyl orange waste water using a three-dimensional electrode reactor, *J. Environ. Sci.*, 2011, **23**, S70-S73.

107. X. Yu, M. Zhou, Y. Hu, K. Groenen Serrano and F. Yu, Recent updates on electrochemical degradation of bio-refractory organic pollutants using BDD anode: a mini review, *Environ. Sci. Pollut. Res. Int.*, 2014, **21**, 8417-8431.

108. B. P. Chaplin, Advantages, Disadvantages, and Future Challenges of the Use of Electrochemical Technologies for Water and Wastewater Treatment, in *Electrochemical Water and Wastewater Treatment*, 2018, DOI: 10.1016/b978-0-12-813160-2.00017-1, pp. 451-494.

109. P. Yao, X. Chen, H. Wu and D. Wang, Active Ti/SnO_2 anodes for pollutants oxidation prepared using chemical vapor deposition, *Surf. Coat. Tech.*, 2008, **202**, 3850-3855.

110. Y. T. Seiya Suzuki, Masamichi Yoshimura, Suppression of Graphene Nucleation by Turning Off Hydrogen Supply Just before Atmospheric Pressure Chemical Vapor Deposition Growth, *Coatings*, 2017, **7**.

111. S. J. Cobb, Z. J. Ayres and J. V. Macpherson, Boron Doped Diamond: A Designer Electrode Material for the Twenty-First Century, *Annu Rev Anal Chem (Palo Alto Calif)*, 2018, **11**, 463-484.

112. F. L. Souza, C. Saéz, M. R. V. Lanza, P. Cañizares and M. A. Rodrigo, The effect of the sp3/sp2 carbon ratio on the electrochemical oxidation of 2,4-D with p-Si BDD anodes, *Electrochim. Acta*, 2016, **187**, 119-124.

113. S. Garcia-Segura, E. Vieira dos Santos and C. A. Martínez-Huitle, Role of sp3/sp2 ratio on the electrocatalytic properties of boron-doped diamond electrodes: A mini review, *Electrochem. Commun.*, 2015, **59**, 52-55.

114. D. Medeiros de Araújo, P. Cañizares, C. A. Martínez-Huitle and M. A. Rodrigo, Electrochemical conversion/combustion of a model organic pollutant on BDD anode: Role of sp 3 /sp 2 ratio, *Electrochem. Commun.*, 2014, **47**, 37-40.

115. E. Guinea, F. Centellas, E. Brillas, P. Cañizares, C. Sáez and M. A. Rodrigo, Electrocatalytic properties of diamond in the oxidation of a persistant pollutant, *Appl. Catal. B-Environ.*, 2009, **89**, 645-650.

116. S. Chai, Y. Wang, Y. N. Zhang, M. Liu, Y. Wang and G. Zhao, Selective Electrocatalytic Degradation of Odorous Mercaptans Derived from S-Au Bond Recongnition on a Dendritic Gold/Boron-Doped Diamond Composite Electrode, *Environ. Sci. Technol.*, 2017, **51**, 8067-8076.

117. K. Muzyka, J. Sun, T. H. Fereja, Y. Lan, W. Zhang and G. Xu, Boron-doped diamond: current progress and challenges in view of electroanalytical applications, *Anal. Methods*, 2019, **11**, 397-414.

118. A. Urtiaga, C. Fernandez-Gonzalez, S. Gomez-Lavin and I. Ortiz, Kinetics of the electrochemical mineralization of perfluorooctanoic acid on ultrananocrystalline boron doped conductive diamond electrodes, *Chemosphere*, 2015, **129**, 20-26.

119. J.-Y. Bak, C.-H. Lee, J.-D. Kim and D.-S. Lim, Modification of the surface morphology of the silicon substrate for boron-doped diamond electrodes in electrochemical wastewater treatment applications, *J. Korean Phys. Soc.*, 2016, **68**, 109-114.

120. M. Brycht, P. Lochyński, J. Barek, S. Skrzypek, K. Kuczewski and K. Schwarzova-Peckova, Electrochemical study of 4-chloro-3-methylphenol on anodically pretreated boron-doped diamond electrode in the absence and presence of a cationic surfactant, *J. Electroanal. Chem.*, 2016, **771**, 1-9.

121. C. Chen, E. Nurhayati, Y. Juang and C. Huang, Electrochemical decolorization of dye wastewater by surface-activated boron-doped nanocrystalline diamond electrode, *J. Environ. Sci. (China)*, 2016, **45**, 100-107.

122. Y. He, X. Wang, W. Huang, R. Chen, H. Lin and H. Li, Application of porous boron-doped diamond electrode towards electrochemical mineralization of triphenylmethane dye, *J. Electroanal. Chem.*, 2016, **775**, 292-298.

123. Y. He, H. Lin, Z. Guo, W. Zhang, H. Li and W. Huang, Recent developments and advances in boron-doped diamond electrodes for electrochemical oxidation of organic pollutants, *Sep. Purif. Technol.*, 2019, **212**, 802-821.

124. T. A. Kenova, G. V. Kornienko, O. A. Golubtsova, V. L. Kornienko and N. G. Maksimov, Electrochemical degradation of Mordant Blue 13 azo dye using boron-doped diamond and

dimensionally stable anodes: influence of experimental parameters and water matrix, *Environ. Sci. Pollut. Res. Int.*, 2018, **25**, 30425-30440.

125. J. F. Carneiro, J. M. Aquino, A. J. Silva, J. C. Barreiro, Q. B. Cass and R. C. Rocha-Filho, The effect of the supporting electrolyte on the electrooxidation of enrofloxacin using a flow cell with a BDD anode: Kinetics and follow-up of oxidation intermediates and antimicrobial activity, *Chemosphere*, 2018, **206**, 674-681.

126. C. Salazar, N. Contreras, H. D. Mansilla, J. Yanez and R. Salazar, Electrochemical degradation of the antihypertensive losartan in aqueous medium by electro-oxidation with boron-doped diamond electrode, *J. Hazard. Mater.*, 2016, **319**, 84-92.

127. I. F. Mena, S. Cotillas, E. Díaz, C. Sáez, Á. F. Mohedano and M. A. Rodrigo, Influence of the supporting electrolyte on the removal of ionic liquids by electrolysis with diamond anodes, *Catal. Today*, 2018, **313**, 203-210.

128. Y. Lan, C. Coetsier, C. Causserand and K. Groenen Serrano, On the role of salts for the treatment of wastewaters containing pharmaceuticals by electrochemical oxidation using a boron doped diamond anode, *Electrochim. Acta*, 2017, **231**, 309-318.

129. C. M. Dominguez, N. Oturan, A. Romero, A. Santos and M. A. Oturan, Removal of lindane wastes by advanced electrochemical oxidation, *Chemosphere*, 2018, **202**, 400-409.

130. Y. Lan, C. Coetsier, C. Causserand and K. Groenen Serrano, An experimental and modelling study of the electrochemical oxidation of pharmaceuticals using a boron-doped diamond anode, *Chem. Eng. J.*, 2018, **333**, 486-494.

131. G. Loos, T. Scheers, K. Van Eyck, A. Van Schepdael, E. Adams, B. Van der Bruggen, D. Cabooter and R. Dewil, Electrochemical oxidation of key pharmaceuticals using a boron doped diamond electrode, *Sep. Purif. Technol.*, 2018, **195**, 184-191.

132. H. Lebik-Elhadi, Z. Frontistis, H. Ait-Amar, S. Amrani and D. Mantzavinos, Electrochemical oxidation of pesticide thiamethoxam on boron doped diamond anode: Role of operating parameters and matrix effect, *Process Saf. Environ.*, 2018, **116**, 535-541.

133. F. C. Moreira, R. A. R. Boaventura, E. Brillas and V. J. P. Vilar, Electrochemical advanced oxidation processes: A review on their application to synthetic and real wastewaters, *Appl. Catal. B-Environ.*, 2017, **202**, 217-261.

134. M. Tang, A. Yuan and J. Xu, Synthesis of highly crystalline $LiMn_2O_4$/multiwalled carbon nanotube composite material with high performance as lithium-ion battery cathode via an improved two-step approach, *Electrochim. Acta*, 2015, **166**, 244-252.

135. Z. Niu, Y. Wang, H. Lin, F. Jin, Y. Li and J. Niu, Electrochemically enhanced removal of perfluorinated compounds (PFCs) from aqueous solution by CNTs-graphene composite electrode, *Chem. Eng. J.*, 2017, **328**, 228-235.

136. X. Zhu, J. Ni, X. Xing, H. Li and Y. Jiang, Synergies between electrochemical oxidation and activated carbon adsorption in three-dimensional boron-doped diamond anode system, *Electrochim. Acta*, 2011, **56**, 1270-1274.

137. N. L. Pedersen, M. Nikbakht Fini, P. K. Molnar and J. Muff, Synergy of combined adsorption and electrochemical degradation of aqueous organics by granular activated carbon particulate electrodes, *Sep. Purif. Technol.*, 2019, **205**, 51-58.

138. J. Mora-Gomez, E. Ortega, S. Mestre, V. Pérez-Herranz and M. García-Gabaldón, Electrochemical degradation of norfloxacin using BDD and new Sb-doped SnO_2 ceramic anodes in an electrochemical reactor in the presence and absence of a cation-exchange membrane, *Sep. Purif. Technol.*, 2019, **208**, 68-75.

139. A. Pieczyńska, T. Ossowski, R. Bogdanowicz and E. Siedlecka, Electrochemical degradation of textile dyes in a flow reactor: effect of operating conditions and dyes chemical structure, *Int. J. Environ. Sci. Technol.*, 2019, **16**, 929-942.

140. B. Gomez-Ruiz, N. Diban and A. Urtiaga, Comparison of microcrystalline and ultrananocrystalline boron doped diamond anodes: Influence on perfluorooctanoic acid electrolysis, *Sep. Purif. Technol.*, 2019, **208**, 169-177.

141. B. Gomez-Ruiz, S. Gómez-Lavín, N. Diban, V. Boiteux, A. Colin, X. Dauchy and A. Urtiaga, Efficient electrochemical degradation of poly- and perfluoroalkyl substances (PFASs) from the effluents of an industrial wastewater treatment plant, *Chem. Eng. J.*, 2017, **322**, 196-204.

142. A. Xue, Z. W. Yuan, Y. Sun, A. Y. Cao and H. Z. Zhao, Electro-oxidation of perfluorooctanoic acid by carbon nanotube sponge anode and the mechanism, *Chemosphere*, 2015, **141**, 120-126.

143. A. L. Valenzuela, R. Vasquez-Medrano, J. G. Ibanez, B. A. Frontana-Uribe and D. Prato-Garcia, Remediation of Diquat-Contaminated Water by Electrochemical Advanced Oxidation Processes Using Boron-Doped Diamond (BDD) Anodes, *Water Air Soil Pollut*, 2017, **228**, 67.

144. D. Shao, W. Yan, X. Li, H. Yang and H. Xu, A Highly Stable Ti/TiH_x/Sb-SnO_2 Anode: Preparation, Characterization and Application, *Ind. Eng. Chem. Res.*, 2014, **53**, 3898-3907.

145. GN Martelli, R Ornelas and G. Faita, Deactivation mechanisms of oxygen evolving anodes at high current densities, *Electrochim. Acta*, 1994, **39**, 1551-1558.

146. W. Yang, W. Yang and X. Lin, Research on PEG modified Bi-doping lead dioxide electrode and mechanism, *Appl. Surf. Sci.*, 2012, **258**, 5716-5722.

147. Y. Q. Wang, B. Gu and W. L. Xu, Electro-catalytic degradation of phenol on several metal-oxide anodes, *J. Hazard. Mater.*, 2009, **162**, 1159-1164.

148. W. Wu, Z.-H. Huang and T.-T. Lim, Recent development of mixed metal oxide anodes for electrochemical oxidation of organic pollutants in water, *Appl. Catal. A- Gen.*, 2014, **480**, 58-78.

149. Zanta, C.L., Michaud, P.A., Comninellis, C., De Andrade, A.R. and Boodts, J.F.,, Electrochemical oxidation of p-chlorophenol on SnO_2-Sb_2O_5 based anodes for wastewater treatment, *J. Appl. Electrochem.*, 2003, **33**, 1211-1215.

150. Y. Samet, S. C. Elaoud, S. Ammar and R. Abdelhedi, Electrochemical degradation of 4-chloroguaiacol for wastewater treatment using PbO_2 anodes, *J. Hazard. Mater.*, 2006, **138**, 614-619.

151. T. Ochiai, Y. Iizuka, K. Nakata, T. Murakami, D. A. Tryk, A. Fujishima, Y. Koide and Y. Morito, Efficient electrochemical decomposition of perfluorocarboxylic acids by the use of a boron-doped diamond electrode, *Diam. Relat. Mater.*, 2011, **20**, 64-67.

152. S. Garcia-Segura, J. D. Ocon and M. N. Chong, Electrochemical oxidation remediation of real wastewater effluents - A review, *Process Saf. Environ.*, 2018, **113**, 48-67.

153. A. De Battisti and C. A. Martínez-Huitle, Electrocatalysis in Wastewater Treatment, in *Electrochemical Water and Wastewater Treatment*, 2018, DOI: 10.1016/b978-0-12-813160-2.00005-5, pp. 119-131.

154. C. E. Schaefer, C. Andaya, A. Burant, C. W. Condee, A. Urtiaga, T. J. Strathmann and C. P. Higgins, Electrochemical treatment of perfluorooctanoic acid and perfluorooctane sulfonate: Insights into mechanisms and application to groundwater treatment, *Chem. Eng. J.*, 2017, **317**, 424-432.

155. M. A. Rodrigo, P. A. Michaud, I. Duo, M. Panizza, G. Cerisola and C. Comninellis, Oxidation of 4-Chlorophenol at Boron-Doped Diamond Electrode for Wastewater Treatment, *J. Electrochem. Soc.*, 2001, **148,** D60-D64.

156. C. Comninellis, Electrocatalysis in the electrochemical conversion/combustion of organic pollutants for waste water treatment, *Electrochim. Acta*, 1994, **39**, 1857-1862.

157. S. Garcia-Segura, J. Keller, E. Brillas and J. Radjenovic, Removal of organic contaminants from secondary effluent by anodic oxidation with a boron-doped diamond anode as tertiary treatment, *J. Hazard. Mater.*, 2015, **283**, 551-557.

158. A. Sánchez-Carretero, C. Sáez, P. Cañizares and M. A. Rodrigo, Electrochemical production of perchlorates using conductive diamond electrolyses, *Chem. Eng. J.*, 2011, **166**, 710-714.

159. S. Vasilie, F. Manea, A. Baciu and A. Pop, Dual use of boron-doped diamond electrode in antibiotics-containing water treatment and process control, *Process Saf. Environ.*, 2018, **117**, 446-453.

160. L. W. Matzek, M. J. Tipton, A. T. Farmer, A. D. Steen and K. E. Carter, Understanding electrochemically activated persulfate and its application to ciprofloxacin abatement, *Environ. Sci. Technol.*, 2018, **52**, 5875-5883.

161. L. W. Matzek and K. E. Carter, Activated persulfate for organic chemical degradation: A review, *Chemosphere*, 2016, **151**, 178-188.

162. J. Radjenovic and M. Petrovic, Sulfate-mediated electrooxidation of X-ray contrast media on boron-doped diamond anode, *Water Res.*, 2016, **94**, 128-135.

163. A. Farhat, J. Keller, S. Tait and J. Radjenovic, Removal of persistent organic contaminants by electrochemically activated sulfate, *Environ. Sci. Technol.*, 2015, **49**, 14326-14333.

164. C. A. Martínez-Huitle and L. S. Andrade, Electrocatalysis in wastewater treatment: recent mechanism advances, *Quím. Nova*, 2011, **34**, 850-858.

165. J. Niu, H. Lin, J. Xu, H. Wu and Y. Li, Electrochemical mineralization of perfluorocarboxylic acids (PFCAs) by ce-doped modified porous nanocrystalline PbO_2 film electrode, *Environ. Sci. Technol.*, 2012, **46**, 10191-10198.

166. S. Li, G. Zhang, W. Zhang, H. Zheng, W. Zhu, N. Sun, Y. Zheng and P. Wang, Microwave enhanced Fenton-like process for degradation of perfluorooctanoic acid (PFOA) using Pb-$BiFeO_3$/rGO as heterogeneous catalyst, *Chem. Eng. J.*, 2017, **326**, 756-764.

167. B. P. Chaplin, Critical review of electrochemical advanced oxidation processes for water treatment applications, *Environ. Sci. Process Impacts*, 2014, **16**, 1182-1203.

168. C. Comninellis, G. Chen, *Electrochemistry for the Environment*, 2010.

169. W. He, Y. Lou, E. Verlato, I. Soutrel, D. Floner, F. Fourcade, A. Amrane, M. Musiani and F. Geneste, Reductive dehalogenation of a chloroacetanilide herbicide in a flow electrochemical cell fitted with Ag-modified Ni foams, *J. Chem. Technol. Biotechnol*., 2018, **93**, 1572-1578.

170. A. A. Isse, S. Arnaboldi, C. Durante and A. Gennaro, Reprint of "Electrochemical reduction of organic bromides in 1-butyl-3-methylimidazolium tetrafluoroborate", *J. Electroanal. Chem.*, 2018, **819**, 562-569.

171. B. A. Walker, E. T. Martin, M. S. Mubarak and D. G. Peters, Electrochemical reduction of dihalothiophenes at silver cathodes in dimethylformamide: Evidence for a halogen dance, *J. Electroanal. Chem.*, 2018, **808**, 335-339.

172. G.-J. Sui, Q.-L. Sun, D. Wu, W.-J. Meng, H. Wang and J.-X. Lu, Electrocatalytic reduction of $PhCH_2Cl$ on Ag-ZSM-5 zeolite modified electrode, *RSC Adv.*, 2016, **6**, 63493-63496.

173. J. A. Rose, C. M. McGuire, A. M. Hansen, J. A. Karty, M. S. Mubarak and D. G. Peters, Direct Reduction of 1-Bromo-6-chlorohexane and 1-Chloro-6-iodohexane at Silver Cathodes in Dimethylformamide, *Electrochim. Acta*, 2016, **218**, 311-317.

174. H. Ma, T. Ge, Q. Cai, Y. Xu, C. Ma, Catalytic Effect of Silver Cathodes on 3,4,5,6-Tetrachloropicolinic Acid Dechlorination in Aqueous Solutions, *Acta Phys. -Chim. Sin.*, 2016, **32**, 1715-1721.

175. Y. Xu, X. Ding, H. Ma, Y. Chu and C. Ma, Selective hydrodechlorination of 3,5,6-trichloropicolinic acid at an activated silver cathode: Synthesis of 3,5-dichloropicolinic acid, *Electrochim. Acta*, 2015, **151**, 284-288.

176. E. T. Martin, L. M. Strawsine, M. S. Mubarak and D. G. Peters, Direct Reduction of 1,2- and 1,6-Dibromohexane at Silver Cathodes in Dimethylformamide, *Electrochim. Acta*, 2015, **186**, 369-376.

177. O. Lugaresi, H. Encontre, C. Locatelli, A. Minguzzi, A. Vertova, S. Rondinini and C. Comninellis, Gas-phase volatile organic chloride electroreduction: A versatile experimental setup for electrolytic dechlorination and voltammetric analysis, *Electrochem. Commun.*, 2014, **44**, 63-65.

178. A. Brzózka, A. Jeleń, A. M. Brudzisz, M. M. Marzec and G. D. Sulka, Electrocatalytic reduction of chloroform at nanostructured silver electrodes, *Electrochim. Acta*, 2017, **225**, 574-583.

179. B. Vanrenterghem, A. Papaderakis, S. Sotiropoulos, D. Tsiplakides, S. Balomenou, S. Bals and T. Breugelmans, The reduction of benzylbromide at Ag-Ni deposits prepared by galvanic replacement, *Electrochim. Acta*, 2016, **196**, 756-768.

180. C. Durante, V. Perazzolo, L. Perini, M. Favaro, G. Granozzi and A. Gennaro, Electrochemical activation of carbon-halogen bonds: Electrocatalysis at silver/copper nanoparticles, *Appl. Catal. B-Environ.*, 2014, **158-159**, 286-295.

181. P. R. M. Abdirisak A. Isse, and Armando Gennaro, New Insights into Electrocatalysis and Dissociative Electron Transfer Mechanisms: The Case of Aromatic Bromides, *J. Phys. Chem. C*, 2009, **113**, 14983-14992.

182. A. A. Isse, G. Berzi, L. Falciola, M. Rossi, P. R. Mussini and A. Gennaro, Electrocatalysis and electron transfer mechanisms in the reduction of organic halides at Ag, *J. Appl. Electrochem.*, 2009, **39**, 2217-2225.

183. S. Arnaboldi, A. Gennaro, A. A. Isse and P. R. Mussini, The solvent effect on the electrocatalytic cleavage of carbon-halogen bonds on Ag and Au, *Electrochim. Acta*, 2015, **158**, 427-436.

184. Z. He, J. Sun, J. Wei, Q. Wang, C. Huang, J. Chen and S. Song, Effect of silver or copper middle layer on the performance of palladium modified nickel foam electrodes in the 2-chlorobiphenyl dechlorination, *J. Hazard. Mater.*, 2013, **250-251**, 181-189.

185. X. Wei, X. Wan, Z. Sun, J. Miao, R. Zhang and Q. J. Niu, Understanding Electrocatalytic Hydrodechlorination of Chlorophenols on Palladium-Modified Cathode in Aqueous Solution, *ACS Omega*, 2018, **3**, 5876-5886.

186. J. Li, C. Luan, Y. Cui, H. Zhang, L. Wang, H. Wang, Z. Zhang, B. Zhao, H. Zhang, X. Zhang and X. Cheng, Preparation and characterization of palladium/polyaniline/foamed nickel composite electrode for electrocatalytic dechlorination, *Sep. Purif. Technol.*, 2019, **211**, 198-206.

187. Z. Lou, J. Zhou, M. Sun, J. Xu, K. Yang, D. Lv, Y. Zhao and X. Xu, MnO_2 enhances electrocatalytic hydrodechlorination by Pd/Ni foam electrodes and reduces Pd needs, *Chem. Eng. J.*, 2018, **352**, 549-557.

188. L. Lan, Y. Liu, S. Liu, X. Ma, X. Li, Z. Dong and C. Xia, Effect of the supports on catalytic activity of Pd catalysts for liquid-phase hydrodechlorination/hydrogenation reaction, *Environ. Technol.*, 2019, **40**, 1651-1623.

189. C. Jiang, H. Yu, Y. Lu, S. Zhu, Z. Geng, M. Huo and X. Wang, Preparation of spike-like palladium nanoparticle electrode and its dechlorination properties, *Thin Solid Films*, 2018, **664**, 27-32.

190. Z. He, Y. Tong, S. Ni, X. Ye, C. P. Makwarimba, X. Huang, S. Zhang and S. Song, Electrochemically reductive dechlorination of 3,6-dichloropicolinic acid on a palladium/nitrogen-doped carbon/nickel foam electrode, *Electrochim. Acta*, 2018, **292**, 685-696.

191. Y. Wu, L. Gan, S. Zhang, B. Jiang, H. Song, W. Li, Y. Pan and A. Li, Enhanced electrocatalytic dechlorination of para -chloronitrobenzene based on Ni/Pd foam electrode, *Chem. Eng. J.*, 2017, **316**, 146-153.

192. Z. Sun, X. Ma and X. Hu, Electrocatalytic dechlorination of 2,3,5-trichlorophenol on palladium/carbon nanotubes-nafion film/titanium mesh electrode, *Environ. Sci. Pollut. Res. Int.*, 2017, **24**, 14355-14364.

193. Z. He, Q. Jian, J. Tang, T. Xu, J. Xu, Z. Yu, J. Chen and S. Song, Improvement of electrochemical reductive dechlorination of 2,4-dichlorophenoxyacetic acid using palladium catalysts prepared by a pulsed electrodeposition method, *Electrochim. Acta*, 2016, **222**, 488-498.

194. Y. Xu, T. Ge, H. Ma, X. Ding, X. Zhang and Q. Liu, Rh-Pd-alloy catalyzed electrochemical hydrodefluorination of 4-fluorophenol in aqueous solutions, *Electrochim. Acta*, 2018, **270**, 110-119.

195. D. Xu, X. Song, W. Qi, H. Wang and Z. Bian, Degradation mechanism, kinetics, and toxicity investigation of 4-bromophenol by electrochemical reduction and oxidation with Pd–Fe/graphene catalytic cathodes, *Chem. Eng. J.*, 2018, **333**, 477-485.

196. H. S. Zhirong Sun, Xuefeng Wei, Xiang Hu, Electrocatalytic hydrogenolysis of chlorophenols in aqueous solution on $Pd_{58}Ni_{42}$ cathode modified with PPy and SDBS, *Chem. Eng. J.,* 2014, **241**, 433-442.

197. Y. Liu, R. Mao, Y. Tong, H. Lan, G. Zhang, H. Liu and J. Qu, Reductive dechlorination of trichloroacetic acid (TCAA) by electrochemical process over Pd-In/Al_2O_3 catalyst, *Electrochim. Acta*, 2017, **232**, 13-21.

198. Y. Wu, L. Gan, S. Zhang, H. Song, C. Lu, W. Li, Z. Wang, B. Jiang and A. Li, Carbon-nanotube-doped Pd-Ni bimetallic three-dimensional electrode for electrocatalytic hydrodechlorination of 4-chlorophenol: Enhanced activity and stability, *J. Hazard. Mater.*, 2018, **356**, 17-25.

199. G. Jiang, M. Lan, Z. Zhang, X. Lv, Z. Lou, X. Xu, F. Dong and S. Zhang, Identification of Active Hydrogen Species on Palladium Nanoparticles for an Enhanced Electrocatalytic

Hydrodechlorination of 2,4-Dichlorophenol in Water, *Environ. Sci. Technol.*, 2017, **51**, 7599-7605.

200. A. Ourari, B. Ketfi, S. I. R. Malha and A. Amine, Electrocatalytic reduction of nitrite and bromate and their highly sensitive determination on carbon paste electrode modified with new copper Schiff base complex, *J. Electroanal. Chem.*, 2017, **797**, 31-36.

201. E. T. Martin, A. L. Goodson, C. M. McGuire, J. A. Rose, A. Ourari, M. S. Mubarak and D. G. Peters, Catalytic reduction of 1-bromodecane and 1-iododecane by electrogenerated, structurally modified nickel(I) salen, *J. Electroanal. Chem.*, 2018, **815**, 225-230.

202. B. H. R. Gerroll, S. P. Bird, E. T. Martin, M. S. Mubarak and D. G. Peters, Cyclohexyl Bromide and Iodide: Direct Reduction at Vitreous Carbon Cathodes together with Nickel(I) Salen- and Cobalt(I) Salen-Catalyzed Reductions in Dimethylformamide, *ChemElectroChem*, 2018, **5**, 902-910.

203. E. R. Wagoner, C. P. Baumberger, B. H. R. Gerroll and D. G. Peters, Catalytic reduction of 1,2,5,6,9,10-hexabromocyclododecane by nickel(I) salen electrogenerated at vitreous carbon cathodes in dimethylformamide, *Electrochim. Acta*, 2014, **132**, 545-550.

204. A. Ourari, Y. Ouennoughi, D. Aggoun, M. S. Mubarak, E. M. Pasciak and D. G. Peters, Synthesis, characterization, and electrochemical study of a new tetradentate nickel(II)-Schiff base complex derived from ethylenediamine and 5′-(N-methyl-N-phenylaminomethyl)-2′-hydroxyacetophenone, *Polyhedron*, 2014, **67**, 59-64.

205. W. Cheng and R. G. Compton, Quantifying the Electrocatalytic Turnover of Vitamin B12-Mediated Dehalogenation on Single Soft Nanoparticles, *Angew. Chem. Int. Ed. Engl.*, 2016, **55**, 2545-2549.

206. H. Shimakoshi and Y. Hisaeda, Electrochemistry and catalytic properties of vitamin B12 derivatives in nonaqueous media, *Curr. Opin. Electrochem.*, 2018, **8**, 24-30.

207. L. Ji, C. Wang, S. Ji, K. P. Kepp and P. Paneth, Mechanism of Cobalamin-Mediated Reductive Dehalogenation of Chloroethylenes, *ACS Catal.*, 2017, **7**, 5294-5307.

208. G. W. Bishop, J. A. Karty and D. G. Peters, Catalytic Reduction of 1,1,1-Trichloro-2,2,2-trifluoroethane (CFC-113a) by Cobalt(I) Salen Electrogenerated at Vitreous Carbon Cathodes in Dimethylformamide, *J. Electrochem. Soc.*, 2007, **154**.

209. M.-A. N. Nguyen, M. E. Tomasso, D. C. Easter and C. Ji, Reaction of Electrogenerated Ligand-Reduced Nickel Salen with Benzyl Bromide, 1-Bromomethylnaphthalene, and α-Bromodiphenylmethane: A Study of Steric Effects, *J. Electrochem. Soc.*, 2015, **163**, G1-G6.

210. E. R. Wagoner, J. A. Karty and D. G. Peters, Catalytic reduction of 4,4′-(2,2,2-trichloroethane-1,1-diyl)bis(chlorobenzene) (DDT) with nickel(I) salen electrogenerated at vitreous carbon cathodes in dimethylformamide, *J. Electroanal. Chem.*, 2013, **706**, 55-63.

211. M. P. Foley, P. Du, K. J. Griffith, J. A. Karty, M. S. Mubarak, K. Raghavachari and D. G. Peters, Electrochemistry of substituted salen complexes of nickel(II): Nickel(I)-catalyzed reduction of alkyl and acetylenic halides, *J. Electroanal. Chem.*, 2010, **647**, 194-203.

212. A. A. Isse, L. Scarpa, C. Durante and A. Gennaro, Reductive cleavage of carbon-chlorine bonds at catalytic and non-catalytic electrodes in 1-butyl-3-methylimidazolium tetrafluoroborate, *Phys. Chem. Chem. Phys.*, 2015, **17**, 31228-31236.

213. K. S. Chan, C. R. Liu and K. L. Wong, Cobalt porphyrin catalyzed hydrodehalogenation of aryl bromides with KOH, *Tetrahedron Lett.*, 2015, **56**, 2728-2731.

214. Z. Sun, X. Wei, H. Shen and X. Hu, Preparation and evaluation of Pd/polymeric pyrrole-sodium lauryl sulfonate/foam-Ni electrode for 2,4-dichlorophenol dechlorination in aqueous solution, *Electrochim. Acta*, 2014, **129**, 433-440.

215. Y. L. Chen, L. Xiong, X. N. Song, W. K. Wang, Y. X. Huang and H. Q. Yu, Electrocatalytic hydrodehalogenation of atrazine in aqueous solution by Cu@Pd/Ti catalyst, *Chemosphere*, 2015, **125**, 57-63.

216. C. Sun, S. A. Baig, Z. Lou, J. Zhu, Z. Wang, X. Li, J. Wu, Y. Zhang and X. Xu, Electrocatalytic dechlorination of 2,4-dichlorophenoxyacetic acid using nanosized titanium nitride doped palladium/nickel foam electrodes in aqueous solutions, *Appl. Catal. B-Environ.*, 2014, **158-159**, 38-47.

217. R. Mao, N. Li, H. Lan, X. Zhao, H. Liu, J. Qu and M. Sun, Dechlorination of Trichloroacetic Acid Using a Noble Metal-Free Graphene-Cu Foam Electrode via Direct Cathodic Reduction and Atomic H, *Environ. Sci. Technol.*, 2016, **50**, 3829-3837.

218. Z. Chen, X. Duan, W. Wei, S. Wang and B.-J. Ni, Recent Advances in Transition Metal-Based Electrocatalysts for Alkaline Hydrogen Evolution, *J. Mater. Chem. A*, 2019, DOI: 10.1039/c9ta03220g.

219. F. Wang, Y. Sun, Y. He, L. Liu, J. Xu, X. Zhao, G. Yin, L. Zhang, S. Li and Q. Mao, Highly efficient and durable MoNiNC catalyst for hydrogen evolution reaction, *Nano Energy*, 2017, **37**, 1-6.

220. R. Liu, H. Zhao, X. Zhao, Z. He, Y. Lai, W. Shan, D. Bekana, G. Li and J. Liu, Defect Sites in Ultrathin Pd Nanowires Facilitate the Highly Efficient Electrochemical Hydrodechlorination of Pollutants by H^*_{ads}, *Environ. Sci. Technol.,* 2018, **52**, 9992-10002.

221. W. Fu, K. Wang, X. Lv, H. Fu, X. Dong, L. Chen, X. Zhang, G. Jiang, Palladium nanoparticles assembled on titanium nitride for enhanced electrochemical hydrodechlorination of 2,4-dichlorophenol in water, *Chinese J. Catal.*, 2018, **39,** 693-700.

222. R. Mao, H. Lan, L. Yan, X. Zhao, H. Liu and J. Qu, Enhanced indirect atomic H* reduction at a hybrid Pd/graphene cathode for electrochemical dechlorination under low negative potentials, *Environ. Sci- Nano*, 2018, **5**, 2282-2292.

223. G. Jiang, K. Wang, J. Li, W. Fu, Z. Zhang, G. Johnson, X. Lv, Y. Zhang, S. Zhang and F. Dong, Electrocatalytic hydrodechlorination of 2,4-dichlorophenol over palladium nanoparticles and its pH-mediated tug-of-war with hydrogen evolution, *Chem. Eng. J.*, 2018, **348**, 26-34.

224. R. Dewil, D. Mantzavinos, I. Poulios and M. A. Rodrigo, New perspectives for Advanced Oxidation Processes, *J. Environ. Manage.*, 2017, **195**, 93-99.

225. E. Brillas and I. Sirés, Hybrid and Sequential Chemical and Electrochemical Processes for Water Decontamination, in *Electrochemical Water and Wastewater Treatment*, 2018, DOI: 10.1016/b978-0-12-813160-2.00011-0, pp. 267-304.

226. W. L. Jiang, X. Xia, J. L. Han, Y. C. Ding, M. R. Haider and A. J. Wang, Graphene Modified Electro-Fenton Catalytic Membrane for in Situ Degradation of Antibiotic Florfenicol, *Environ. Sci. Technol.*, 2018, **52**, 9972-9982.

227. K. Yang, H. Lin, S. Liang, R. Xie, S. Lv, J. Niu, J. Chen and Y. Hu, A reactive electrochemical filter system with an excellent penetration flux porous Ti/SnO_2-Sb filter for efficient contaminant removal from water, *RSC Adv.*, 2018, **8**, 13933-13944.

228. S. Xu, J. Zheng, Z. Wu, M. Liu and Z. Wang, Degradation of p-chloroaniline using an electrochemical ceramic microfiltration membrane with built-in electrodes, *Electrochim. Acta*, 2018, **292**, 655-666.

229. L. Chen, J. Shao, H. Chen, C. Wang, X. Gao, X. Xu and L. Zhu, Cathode potential regulation in a coupled bioelectrode-anaerobic sludge system for effective dechlorination of 2,4-dichloronitrobenzene, *Bioresour. Technol.*, 2018, **254**, 180-186.

230. S. Cotillas, D. Clematis, P. Canizares, M. P. Carpanese, M. A. Rodrigo and M. Panizza, Degradation of dye Procion Red MX-5B by electrolytic and electro-irradiated technologies using diamond electrodes, *Chemosphere*, 2018, **199**, 445-452.

231. S. Wohlmuth da Silva, A. N. Arenhart Heberle, A. Pereira Santos, M. A. Siqueira Rodrigues, V. Perez-Herranz and A. Moura Bernardes, Antibiotics mineralization by electrochemical and UV-based hybrid processes: evaluation of the synergistic effect, *Environ. Technol.*, 2018, DOI: 10.1080/09593330.2018.1478453, 1-11.

232. C. Rosales Landeros, C. E. Barrera Díaz, A. Amaya Cháves and G. Roa Morales, Evaluation of a coupled system of electro-oxidation and ozonation to remove the pesticide Thiodan® 35 CE (endosulfan) in aqueous solution, *Fuel*, 2017, **198**, 91-98.

233. Q. Huang, S. Deng, D. Shan, Y. Wang, B. Wang, J. Huang and G. Yu, Enhanced adsorption of diclofenac sodium on the carbon nanotubes-polytetrafluorethylene electrode and subsequent degradation by electro-peroxone treatment, *J. Colloid Interface Sci.*, 2017, **488**, 142-148.

234. M. Shestakova, M. Vinatoru, T. J. Mason and M. Sillanpaa, Sonoelectrocatalytic decomposition of methylene blue using Ti/Ta_2O_5-SnO_2 electrodes, *Ultrason. Sonochem.*, 2015, **23**, 135-141.

235. J. M. Aquino, D. W. Miwa, M. A. Rodrigo and A. J. Motheo, Treatment of actual effluents produced in the manufacturing of atrazine by a photo-electrolytic process, *Chemosphere*, 2017, **172**, 185-192.

236. N. Wang and P. Wang, Study and application status of microwave in organic wastewater treatment - A review, *Chem. Eng. J.*, 2016, **283**, 193-214.

237. H. Xiao, B. Lv, J. Gao and G. Zhao, Hydrothermal electrocatalytic oxidation for the treatment of herbicides wastewater, *Environ. Sci. Pollut. Res. Int.*, 2016, **23**, 10050-10057.

238. H. Xiao, B. Lv, G. Zhao, Y. Wang, M. Li and D. Li, Hydrothermally enhanced electrochemical oxidation of high concentration refractory perfluorooctanoic acid, *J. Phys. Chem. A*, 2011, **115**, 13836-13841.

239. P. Gayen, C. Chen, J. T. Abiade and B. P. Chaplin, Electrochemical Oxidation of Atrazine and Clothianidin on Bi-doped SnO_2-Ti_nO_{2n-1} Electrocatalytic Reactive Electrochemical Membranes, *Environ. Sci. Technol.*, 2018, **52**, 12675-12684.

240. A. Soriano, D. Gorri and A. Urtiaga, Efficient treatment of perfluorohexanoic acid by nanofiltration followed by electrochemical degradation of the NF concentrate, *Water Res.*, 2017, **112**, 147-156.

241. A. Bedolla-Guzman, R. Feria-Reyes, S. Gutierrez-Granados and J. M. Peralta-Hernandez, Decolorization and degradation of reactive yellow HF aqueous solutions by electrochemical advanced oxidation processes, *Environ. Sci. Pollut. Res. Int.*, 2017, **24**, 12506-12514.

242. Y. Wang, X. Zhang, H. Feng, Y. Liang, D. Shen, Y. Long, Y. Zhou and Q. Dai, Biocatalysis mechanism for p-fluoronitrobenzene degradation in the thermophilic bioelectrocatalysis system: Sequential combination of reduction and oxidation, *Chemosphere*, 2016, **159**, 44-49.

243. K. Zhu, C. Sun, H. Chen, S. A. Baig, T. Sheng and X. Xu, Enhanced catalytic hydrodechlorination of 2,4-dichlorophenoxyacetic acid by nanoscale zero valent iron with

electrochemical technique using a palladium/nickel foam electrode, *Chem. Eng. J.*, 2013, **223**, 192-199.

244. N. Oturan, E. D. van Hullebusch, H. Zhang, L. Mazeas, H. Budzinski, K. Le Menach and M. A. Oturan, Occurrence and Removal of Organic Micropollutants in Landfill Leachates Treated by Electrochemical Advanced Oxidation Processes, *Environ. Sci. Technol.*, 2015, **49**, 12187-12196.

245. N. Oturan and M. A. Oturan, Electro-Fenton Process: Background, New Developments, and Applications, in *Electrochemical Water and Wastewater Treatment*, 2018, DOI: 10.1016/b978-0-12-813160-2.00008-0, pp. 193-221.

246. P. A. Reddy, P. V. Reddy, E. Kwon, K. H. Kim, T. Akter and S. Kalagara, Recent advances in photocatalytic treatment of pollutants in aqueous media, *Environ. Int.*, 2016, **91**, 94-103.

247. C. Baldisserri, S. Ortelli, M. Blosi and A. L. Costa, Pilot- plant study for the photocatalytic/electrochemical degradation of Rhodamine B, *J. Environ. Chem.Eng.*, 2018, **6**, 1794-1804.

248. N. Jaafarzadeh, G. Barzegar and F. Ghanbari, Photo assisted electro-peroxone to degrade 2,4-D herbicide: The effects of supporting electrolytes and determining mechanism, *Process Saf. Environ.*, 2017, **111**, 520-528.

249. F. L. Souza, C. Sáez, P. Cañizares, A. J. Motheo and M. A. Rodrigo, Coupling photo and sono technologies to improve efficiencies in conductive diamond electrochemical oxidation, *Appl. Catal. B-Environ.*, 2014, **144**, 121-128.

250. L. Huang, S. Cheng and G. Chen, Bioelectrochemical systems for efficient recalcitrant wastes treatment, *J. Chem. Technol. Biot.*, 2011, **86**, 481-491.

251. M. Zhou, H. Wang, D. J. Hassett and T. Gu, Recent advances in microbial fuel cells (MFCs) and microbial electrolysis cells (MECs) for wastewater treatment, bioenergy and bioproducts, *J. Chem. Technol. Biot*, 2013, **88**, 508-518.

252. M. Solís, A. Solís, H. I. Pérez, N. Manjarrez and M. Flores, Microbial decolouration of azo dyes: A review, *Process Biochem.*, 2012, **47**, 1723-1748.

253. S. K. Sharma and R. Sanghi, *Advances in Water Treatment and Pollution Prevention*, 2012.

254. C. Dai, Y. Zhou, H. Peng, S. Huang, P. Qin, J. Zhang, Y. Yang, L. Luo and X. Zhang, Current progress in remediation of chlorinated volatile organic compounds: A review, *J. Ind. Eng. Chem.*, 2018, **62**, 106-119.

255. X. Li, H.-Y. Wang, H. Yang, W. Cai, S. Liu and B. Liu, In Situ/Operando Characterization Techniques to Probe the Electrochemical Reactions for Energy Conversion, *Small Methods*, 2018, **2**, 1700395.

256. X. Li, X. Huang, S. Xi, S. Miao, J. Ding, W. Cai, S. Liu, X. Yang, H. Yang, J. Gao, J. Wang, Y. Huang, T. Zhang and B. Liu, Single Cobalt Atoms Anchored on Porous N-Doped Graphene with Dual Reaction Sites for Efficient Fenton-like Catalysis, *J. Am. Chem. Soc.*, 2018, **140**, 12469-12475.

257. C. Zhao, B. Liu, X. Li, K. Zhu, R. Hu, Z. Ao and J. Wang, Co-Fe Prussian blue analogue for efficient Fenton-like catalysis: the effect of high-spin cobalt, *Chem. Commun.*, 2019, DOI: 10.1039/c9cc01872g.

View Article Online
DOI: 10.1039/C9EN00411D

Table of Contents Entry

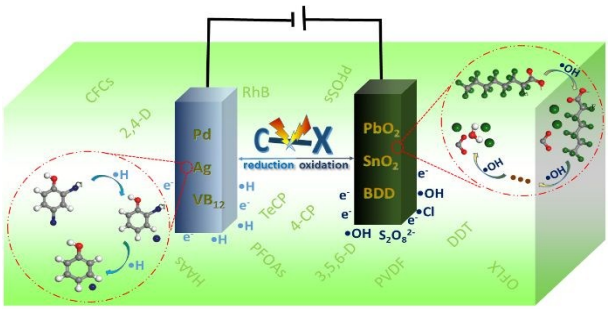

Advanced Electrocatalysts for Halogenated Organic Pollutants Degradation